Received: 14 October 2025 | Accepted: 12 June 2026

DOI: 10.1002/vzj2.70127

Vadose Zone Journal

ORIGINAL ARTICLE

Special Section: Advances in Monitoring Soil Water Content

Toward a structured workflow to harmonize soil water content products: A comparative study across different methods

Sadra Emamalizadeh[1] | **Tim Howson**[2] | **Riccardo Mazzoleni**[1] | **Philip Vincent**[2] | **Jonathan G. Evans**[2] | **Gabriele Baroni**[1]

[1]Department of Agricultural and Food Sciences, University of Bologna, Bologna, Italy

[2]UK Centre for Ecology and Hydrology, Wallingford, UK

Correspondence
Gabriele Baroni, Department of Agricultural and Food Sciences, University of Bologna, Viale G. Fanin 50, Bologna, 40127, Italy. Email: g.baroni@unibo.it

Assigned to Associate Editor Michael Cosh.

Funding information
European Partnership on Metrology, Grant/Award Number: 21GRD08 SoMMet

Abstract

This study introduces a structured, multi-step workflow for harmonizing diverse soil water content (SWC) datasets to improve their meaningful comparability while preserving their intrinsic characteristics. The workflow addresses four components: unit, temporal, vertical, and lateral spatial harmonization, and is applied to point-scale (PS) sensors, cosmic-ray neutron sensing (CRNS), and remote sensing (RS) data from seven European sites. Statistical metrics and physically based plausibility checks using pedotransfer functions define realistic SWC ranges. A literature review of 60 studies identified five methodological classes: general statistical, spatial statistical, machine learning (ML), triple collocation (TC), and process-based models. For unit harmonization, total water capacity conversion outperformed mean-variance matching, improving the proportion of values within the field capacity (FC)–wilting point (WP) range. Temporal harmonization showed negligible differences between daily averaging and satellite overpass selection (<1% for CRNS, ∼16% for PS for both methods). Depth harmonization using weighted averaging and exponential filtering enhanced dataset alignment ($\Delta R = 0.15$, ΔubRMSD [unbiased root mean square deviation $= -0.03$]). For lateral spatial, while simpler methods like areal mean are easy to implement with a single PS sensor, they often fail to preserve the distinct signals. The TC method provides a more robust, error-aware approach for data-scarce sites. ML methods like random forest can capture nonlinearity but risk overfitting and are more applicable to data fusion. More spatially faithful method, ordinary kriging, provided the highest quantitative improvements (FC–WP plausibility +16% for CRNS, +30% for RS). Optimal harmonization is context-dependent, balancing data availability, interpretability, and physical consistency. The proposed framework enhances comparability and traceability across multi-sensor SWC studies.

Abbreviations: BD, bulk density; CDF, cumulative distribution function; CRNS, cosmic-ray neutron sensing; C-band SAR, C-band Synthetic Aperture Radar; FC, field capacity; ML, machine learning; PS, point-scale; PTFs, pedotransfer functions; QC, quality control; RF, random forest; RS, remote sensing; SSM, surface soil moisture; SWC, soil water content; TC, triple collocation; ubRMSD, unbiased root mean square deviation; VWC, volumetric water content; WP, wilting point.

Plain Language Summary

Soils act as a sponge, storing water that plants need and that also regulates floods, droughts, and climate. But different sensors (in-ground probes, cosmic-ray detectors, and satellites) measure soil water differently, making it hard to compare their readings directly. In this work, we present a step-by-step workflow that allows many kinds of soil moisture data to be put on a common footing without "blending" them away. We tested different methods to make their units, timescales, depth profiles, and spatial coverage compatible. We found that some physically based conversions and spatial interpolation techniques greatly improve agreement among the datasets and ensure the harmonized results remain realistic (i.e., within expected soil moisture ranges). The outcome is a clear, traceable process that other scientists can use to combine soil moisture measurements from different sources. This helps researchers use multi-sensor data more reliably in hydrology and agricultural applications.

1 | INTRODUCTION

Soil water content (SWC), or soil moisture, plays a fundamental role in various environmental and hydrological processes. It regulates land–atmosphere interactions (Seneviratne et al., 2010), influences agricultural productivity (D. Wu et al., 2021), affects ecosystem health (L. Liu et al., 2020), and governs hydrological modeling and water resource management (Brocca et al., 2017). Accurate estimation of SWC is crucial for these applications, yet obtaining reliable measurements is challenging due to its high spatial and moderate temporal variability (Mälicke et al., 2020).

Different methods have been developed to estimate SWC at varying scales, each with distinct advantages and limitations. Broadly, SWC measurement techniques can be categorized into three groups based on their spatial coverage: point-scale (PS) sensors, intermediate proximal sensors like cosmic-ray neutron sensing (CRNS), and remote sensing (RS) satellite images (Ochsner et al., 2013). PS sensors, including both static and mobile instruments, provide localized, high-precision measurements but lack extensive coverage (Robinson et al., 2008). Proximal sensing like CRNS offers an intermediate-scale solution, integrating SWC information over a larger footprint (up to hundreds of meters) (Baroni et al., 2018; Bogena et al., 2015; Zreda et al., 2008). RS, on the other hand, provides large-scale observations, enabling regional and global monitoring but often with lower resolution and depth-limited penetration (Peng, Albergel, et al., 2021). Given these differences, direct comparisons between datasets obtained from these methods are not straightforward. When using them for validation, merging, or intercomparison studies, harmonization becomes an essential step to ensure consistency and comparability.

Despite its importance, the concept of harmonization has often been used interchangeably with data fusion in the literature (Castanedo, 2013; Zhao et al., 2024). While both share some similarities, a crucial distinction exists between them. The latter typically aims to integrate multiple datasets into a new product, whereas harmonization, as defined in this study, focuses on making datasets more (meaningfully) comparable while preserving their distinct characteristics. This definition not only provides a structured approach for handling diverse datasets but also helps in method selection. By positioning harmonization as a necessary step after quality control (QC) and before data fusion in the workflow, methodologies that do not align with our definition, such as those that significantly alter the nature of the original dataset rather than improving its comparability, can be excluded.

While various studies have explored harmonization techniques, they often focus on specific aspects without addressing all relevant components comprehensively or assessing the effect of the selected method on the final results. For instance, Usowicz et al. (2020) compared RS and PS with a special focus on penetration depth. Peng, Tanguy et al. (2021) compared several SWC products integrating both unit transformation and seasonal detrending. Schmidt et al. (2024) compared RS and CRNS datasets with the focus on units' transformation, temporal mismatch, and penetration depth. Direct comparison with very brief data preparation is also common (Upadhyaya et al., 2021). This variety of approaches used for the intercomparison of the different SWC products limits the possibility to compare the results across studies and to gain knowledge from the repetition of the assessments at the different locations.

To bridge this gap, in this study, harmonization is categorized into four key components with increasing complexity: unit harmonization, temporal harmonization, vertical harmonization (depth adjustment), and lateral spatial harmonization. A review of 60 relevant studies has been conducted (see Appendix), and those were categorized into five distinct classes: general statistical, spatial statistical, machine learning (ML), triple collocation (TC), and process-based models. For each of the harmonization components, two of the most used and relevant methods were selected to enable a comparative study. Lateral spatial harmonization, due to its complexity and more noticeable presence in the reviewed literature, required more than two methods. To navigate the diverse methodologies encountered for lateral spatial variability, from the previously mentioned general categories, a representative method was selected for application and evaluation, with choices guided by an assessment of the strengths and limitations of each method. This ensured that the selected methods encapsulated the key trade-offs observed in the literature while maintaining alignment with the broader objectives of harmonization.

The approaches have been applied to seven datasets collected at different sites over Europe that comprise PS, CRNS, and RS products. By following this structured approach, our study aims to systematically evaluate harmonization techniques, offering insights into their effectiveness and implications. This framework provides a foundation for more reliable intercomparisons of SWC datasets, improving their usability in hydrological and environmental applications.

Core Ideas

- The total water capacity conversion method for unit harmonization improved the physical plausibility of remote sensing (RS) data, increasing values within field capacity–wilting point ranges by up to 7% compared to mean-variance matching.
- Temporal harmonization methods (daily averaging vs. overpass selection) showed negligible performance differences, confirming that soil water content comparability is not largely affected by sub-daily variability.
- Depth harmonization using weighted averaging (for point-scale sensors) and exponential filtering (for remote sensing product) enhanced remote sensing-ground agreement ($\Delta R = +0.15$, ΔubRMSD $= -0.03$ [ΔubRMSD is unbiased root mean square deviation]) and increased remote sensing dataset plausibility by ~12%.
- For lateral spatial harmonization, ordinary kriging provided the largest quantitative improvement (R +0.43–0.44, field capacity (FC)–wilting point (WP) plausibility +16% for cosmic-ray neutron sensing, +30% for remote sensing) but required large point-scale sensors network; random forest offered large statistical gains as well but risked overfitting.
- The workflow demonstrates that optimal harmonization is context-dependent, with ordinary kriging best for data-rich sites and triple collocation + mean-variance matching most practical for small networks, enhancing cross-sensor comparability and reproducibility.

2 | MATERIALS AND METHODS

2.1 | Study areas and datasets

The study analyzes seven sites across Europe (Figure 1), primarily affiliated with the SoMMet project (https://www.sommet-project.eu) and the COSMOS-UK network (https://cosmos.ceh.ac.uk). UK sites provide the longest observational records (2016–2024), while Italian sites offer shorter data with considerable gaps. These kinds of variable and sometimes sparse datasets are common in real-world applications and must be taken into account when designing and applying harmonization methods. Almost all sites feature at least one PS sensor that includes shallow SWC measurements at 5-cm depth. PS sensor density varies considerably across sites, ranging from 1 PS sensor (Imola) to 30 sensors (Marquadt) within the RS pixel over that field. Because the CRNS data for the Marquadt site are available only at daily resolution, this site is excluded from the initial comparisons and included only after temporal harmonization. Accordingly, the initial analysis focuses on the remaining six sites. Spatially, soil and land use are mostly homogeneous at the CRNS coverage scale but often heterogeneous within coarser resolution RS pixels. Site-specific properties, including soil type, land use within the CRNS footprint, and data availability, are detailed in Table 1.

At the PS, SWC is measured over a very localized volume, typically just a few millimeters or centimeters around the sensor. While these high-resolution data are valuable for site-specific analysis, they pose challenges for broader comparisons, especially during lateral spatial harmonization. Given the potential for variations in PS sensor types and operational characteristics at different sites, more information can be found by consulting the individual site references (Table 1). In some cases, such as Imola, only one sensor was available (Figure 1), highlighting the need for harmonization strategies that adapt to limited data availability. Most sensors recorded data at hourly or sub-hourly intervals; the latter were aggregated using a mean to produce an hourly time series. All measurements are reported in volumetric water content (VWC), with units of m^3/m^3.

CRNS provides an intermediate-scale solution for SWC monitoring, filling the gap between localized PS sensors and broader RS products. The method operates by detecting epithermal neutrons generated from cosmic rays that inter-

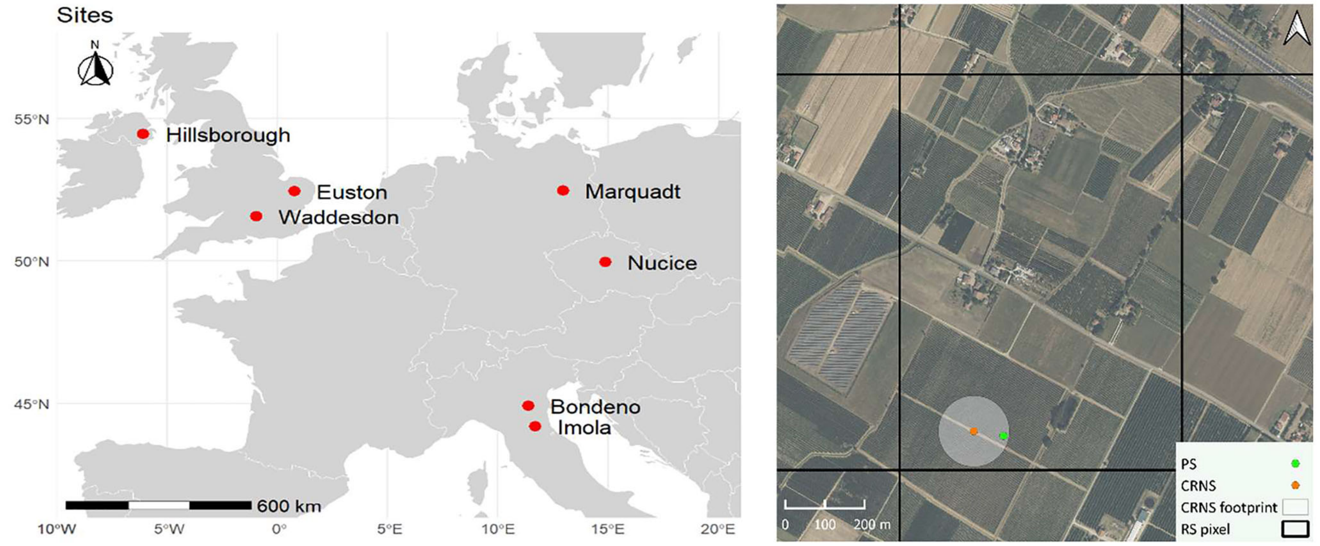

FIGURE 1 Left panel: Geographic locations of the seven study sites across Europe. Right panel: Example from the Imola site showing the 1 km remote sensing [RS] pixel (grid with black segments), cosmic-ray neutron sensing (CRNS) location and its considered footprint (125 m radius, orange point, and gray shaded circle), and point-scale (PS) location (green point). This illustrates the spatial relationship among sensing systems.

TABLE 1 Features of the studied sites.

Site name	Soil type	Land use	PS sensors within RS pixel	PS data period (gaps included)	CRNS data period (gaps included)	Reference
Bondeno	Clay loam	Orchard land	8	July 2024–Sept. 2024	Aug. 2021–Dec. 2024	(Mazzoleni et al., 2025)
Imola	Silty clay loam	Cropland	1	June 2023–Sept. 2023, June 2024–July 2024	Apr. 2023–Oct. 2023	
Marquadt	Sandy loam	Crop/orchard/grassland	30	Dec. 2018–Jan. 2020	July 2019–Nov. 2022 (daily)	(Heistermann et al., 2023)
Nucice	Silt loam	Cropland	2	Mar. 2024–Aug. 2024	Sept. 2022–June 2023	(T. Li et al., 2021)
Euston	Sandy loam	Grassland	2	Apr. 2016–Dec. 2024	Apr. 2016–Dec. 2024	(Cooper et al., 2021)
Waddesdon	Clay loam	Grassland	2	Feb. 2020–Dec. 2024	Jan. 2016–Dec. 2024	
Hillsborough	Sandy loam	Grassland	2	June 2016–Dec. 2024	June 2016–Dec. 2024	

Abbreviations: CRNS, cosmic-ray neutron sensing; PS, point-scale; RS, remote sensing.

act with hydrogen atoms in the soil. Since water contains hydrogen, neutron counts are inversely related to SWC levels. However, raw neutron data require several preprocessing steps, such as corrections for atmospheric pressure, humidity, and incoming neutron flux, to translate them into reliable SWC estimates (Baroni et al., 2018). These preprocessing steps were already applied by the institutions managing each CRNS station using established, sensor-specific processing methods. Standardized open-source frameworks for CRNS data processing, such as CRSPy (Cosmic-Ray neutron Sensor PYthon tool; Power et al., 2021) and CRNPy (Cosmic-ray Neutron Python library; Rud et al., 2024), have been developed to support consistent implementation of these corrections. In this study, such corrections are treated as part of the CRNS SWC retrieval process, analogous to the conversion of satellite backscatter to soil moisture in RS, and are therefore considered a prerequisite rather than an element of the harmonization workflow (Cooper et al., 2021; Heistermann et al., 2023; T. Li et al., 2021). The spatial footprint of CRNS typically ranges from ∼100 to 250 m in radius (Zreda et al., 2012), depending on environmental and soil conditions. In this study, a buffer radius of 125 m (Emamalizadeh et al., 2024), approximately 5 ha, was chosen to represent the area contributing most significantly (~86%) to the CRNS signal under varying SWC states (Schrön et al., 2017). This footprint makes CRNS especially useful for agricultural and hydrological applications at the field scale (Schrön et al., 2017). Its intermediate resolution also allows it to serve as a valuable reference value for both upscaling PS data and downscaling satellite observations (Figure 1). The sensing depth of CRNS is more complex to define, as it decreases with increasing distance from the sensor and is influenced by site-specific factors such as SWC content; in general, it is more sensitive to moisture closer to the sensor and near the surface (Schrön et al., 2017). CRNS data used in this study were recorded hourly and in the VWC unit.

RS products generally offer broad spatial coverage, often with resolutions of several kilometers (Babaeian et al., 2019). This makes them valuable for large-scale monitoring, though their accuracy may suffer compared to in-situ measurements; therefore, there is a need for ground-based comparison and validation. Their temporal resolution is typically limited by satellite revisit cycles; however, with the aid of advanced interpolation techniques and data merging algorithms (Bauer-Marschallinger et al., 2018; X. Zhu et al., 2010), products with improved temporal granularity have become available. In this study, the daily surface soil moisture (SSM) product provided by the Copernicus Land Monitoring Service (Bauer-Marschallinger et al., 2019) was used. This product is derived from Sentinel-1 C-band Synthetic Aperture Radar (C-band SAR) observations and provides surface SWC estimates by applying retrieval models that relate backscattered C-band SAR signals to surface dielectric properties, which are primarily controlled by SWC but are also influenced by surface roughness, vegetation cover and structure, and ancillary surface and soil conditions such as soil temperature. One major reason for selecting this product is its favorable trade-off between spatial and temporal resolution: the 1 km spatial resolution makes it suitable for field-scale applications and better aligned with CRNS data (Figure 1), especially when compared to coarser products with pixels of 25–50 km resolution. At such large scales, the heterogeneity of influencing factors like vegetation cover, soil type, topography, atmospheric conditions, and irrigation zonation (Crow et al., 2012; Emamalizadeh et al., 2024) becomes more pronounced, complicating comparisons with point or field-scale measurements. The SSM product is distributed at a daily temporal resolution, reflecting the temporal availability of processed Sentinel-1 observations. Its sensing depth, similar to other C-band radar-based RS products, is typically confined to the very topsoil layer (approximately 1–2 cm), depending on soil moisture, surface roughness, and vegetation conditions (Ulaby et al., 1996), which aligns well with the depth of PS data used in this study and supports more direct comparisons. Another key consideration is the unit type. Unlike most of the RS products (e.g., SMAP [soil moisture active passive; Entekhabi et al., 2010] and SMOS [soil moisture and ocean salinity; Kerr et al., 2010]), which are expressed in VWC, the SSM product, and a few more (e.g., ASCAT [Wagner et al., 2013]) provide values in relative saturation units (0%–100%). Therefore, unit harmonization is necessary to ensure compatibility with CRNS and PS datasets. This involved applying transformation methods to convert saturation into VWC, enabling consistent cross-dataset analysis. For all sites in our study, the SSM dataset from 2016 to the end of 2024 was used, selecting the pixel covering the central location of the CRNS of each site.

2.2 | Statistical metrics and plausible analysis

Two commonly used statistical metrics were used to quantify agreement between datasets at each harmonization step: the Pearson correlation coefficient (R) and the unbiased root mean square deviation (ubRMSD). The R (Equation 1) captures the strength and direction of the linear relationship between datasets, highlighting how well they align in terms of dynamic fluctuations. The ubRMSD (Equation 2), on the other hand, removes the effect of systematic bias and isolates random discrepancies, making it particularly suitable for assessing harmonization performance. In the equations below, the terms X_i and Y_i correspond to paired observations from the two datasets being compared. The symbols $\bar{X}$ and $\bar{Y}$ represent the arithmetic means of the X and Y datasets, while n denotes the total number of observations in each dataset.

$$R = \frac{\sum_{i=1}^{n} \left(X_i - \bar{X}\right)\left(Y_i - \bar{Y}\right)}{\sqrt{\sum_{i=1}^{n} \left(X_i - \bar{X}\right)^2 \sum_{i=1}^{n} \left(Y_i - \bar{Y}\right)^2}} \tag{1}$$

$$\text{ubRMSD} = \sqrt{\frac{1}{n} \sum_{i=1}^{n} \left[\left(X_i - Y_i\right) - \left(\bar{X} - \bar{Y}\right)\right]^2} \tag{2}$$

Noteworthy, however, some harmonization options might overfit the SWC products, that is, excessively adapt the harmonization to the specific calibration dataset, leading to improved apparent agreement but reduced robustness and transferability across independent conditions and also undermining their different nature. For this reason, better performance should not necessarily be interpreted as better results in the harmonizations. Therefore, in addition to the statistical metrics, hydraulic soil properties have been used to define the plausible range of SWC. This approach is consistent with our definition of harmonization, as datasets are more comparable when they are within physically meaningful intervals. Specifically, field capacity (FC) and wilting point (WP) are considered. The change of proportion of SWC values that fell within this range (between WP and FC) before and after applying a harmonization method, offering a plausibility check for harmonized outputs, is calculated.

For consistency across sites, these thresholds have been estimated by using global soil data and pedotransfer functions (PTFs). Texture and bulk density (BD) data were obtained from SoilGrids (https://soilgrids.org), which provides global estimates of soil properties at a 250-m resolution (Poggio et al., 2021). Although less precise than in-situ measurements, SoilGrids enables harmonized and spatially continuous estimations, making it particularly useful in data-scarce regions. Data were retrieved for depths of 0–5, 5–15, and 15–30 cm, then aggregated both laterally and vertically to align with the respective sensor footprints and various depth ranges. PTFs are empirical models that infer hard-to-measure soil hydraulic parameters from more accessible characteristics such as soil texture and organic matter (Wösten et al., 1999). In this study, we used the euptfv2 model (https://ptfinterface.rissac.hu), an updated European open-access tool that provides predictions across diverse soil types (Szabó et al., 2021) while requiring fewer input parameters than other alternative functions. For consistency across sites, only the essential inputs were used: depth, along with sand, silt, and clay percentages. However, it is important to note that including additional parameters, such as BD and organic carbon content, can enhance the accuracy of the estimates (Szabó et al., 2021). The euptfv2 provides two estimates of FC: FC, which corresponds to a matric potential of −330 cm, and FC2, which corresponds to −100 cm. FC2 was used because initial assessments showed that FC underestimated FC at our study sites, with most sensor data falling outside expected ranges. This finding is supported by Krueger and Ochsner (2024), underscoring that FC generally underestimates SWC, whereas FC2 yields a more reliable approximation.

2.3 | Literature review and harmonization framework

A comprehensive literature review was conducted, covering 60 peer-reviewed articles. These studies were selected using targeted keyword searches such as “Harmonization + soil moisture,” “Soil moisture + upscaling/downscaling,” “Soil moisture + triple collocation,” and “Soil moisture + scaling.” A significant insight from the performed literature review was that most research have concentrated on lateral spatial (area) harmonization (specifically upscaling/downscaling), often embedded within data fusion processes, while other elements of harmonization, such as unit, temporal, and depth, received limited attention. It was observed that the studies can be categorized into five general classes (Figure 2), each representing a specific philosophy or modeling strategy:

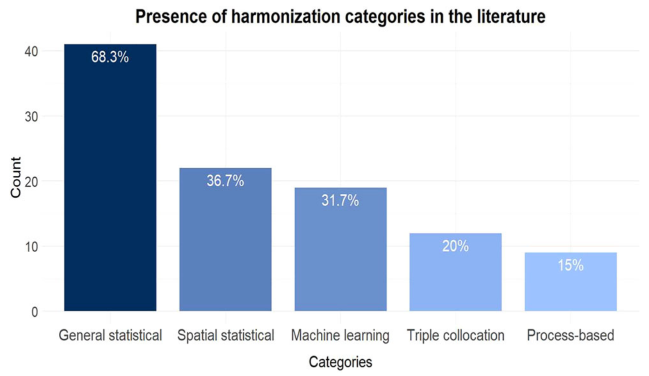

FIGURE 2 Frequency of five harmonization categories in the literature review: general statistical, spatial statistical, machine learning, triple collocation, and process-based. Percentages indicate each method’s presence share in the review.

2.3.1 | General statistical methods

These methods, which account for the highest presence with 41 studies (Figure 2), include straightforward approaches such as ordinary least squares, ridge regression (Kang et al., 2018), and arithmetic mean (also referred to as areal mean or average) (Heathman, Cosh, Han, et al., 2012). They assume linear relationships, are computationally efficient, and work even with minimal data (e.g., a single PS sensor). While useful for quick, preliminary harmonization in data-scarce contexts, they lack spatial modeling and cannot capture nonlinear SWC dynamics, making them low in spatial sophistication.

2.3.2 | Spatial statistical methods

This group includes geostatistical tools like kriging and variogram analysis (Webster & Oliver, 2008). These methods explicitly model spatial dependence through variograms and are ideal for estimating SWC across landscapes when a sufficiently large number of observation locations to allow reliable empirical estimation of the spatial variogram is available (Tunçay, 2021; B. Xie et al., 2020, 2025; Zheng et al., 2009). They maintain natural spatial structure and are especially useful for interpolation within homogeneous zones. However, these models generally rely on an assumption of stationarity, although in practice this assumption is often relaxed through the use of localized search neighborhoods that reduce the influence of non-stationarity.

2.3.3 | ML approaches

ML methods like random forest (RF) (Y. Zhang et al., 2023), k-nearest neighbors (Y. Liu et al., 2017; Seo et al., 2021), neural networks (Seo et al., 2021), and support vector machines (Yan & Bai, 2020) are data-driven and can capture nonlinear interactions and complex spatial patterns in SWC. They require substantial training data and multiple PS sensors, but their "black box" nature limits interpretability. While moderately spatially aware, they are computationally demanding and may overlap with data fusion when overfit.

2.3.4 | TC techniques

TC is a statistical technique used to estimate the random errors of three independent measurement systems without requiring a known "truth" reference (Gruber et al., 2013). Originally introduced in wind scatterometry studies (Stoffelen, 1998), TC has gained traction in SWC harmonization for assessing the reliability of different datasets, for example, Chen et al (2018), Duygu and Akyürek (2019), Gruber et al. (2013), Peng, Tanguy et al. (2021). The core TC equation estimates the error variance of each dataset (σ) based on the covariances among them. In its standard form, it calculates the error variance of one dataset (say, A) as:

$$\sigma^2{}_A = \mathrm{var}(A) - \frac{\mathrm{cov}(A, B) \cdot \mathrm{cov}(A, C)}{\mathrm{cov}(B, C)} \tag{3}$$

where A, B, and C are the three datasets. It is easy to implement (even with one PS sensor), preserves dataset characteristics, and provides objective quality estimates. However, its assumptions (linearity, stationarity, and no correlated errors) may not always hold, so TC is best for diagnosing dataset quality rather than achieving full harmonization, which often requires additional statistical matching.

2.3.5 | Process-based models

Process-based models representing the smallest presence, with nine studies (Figure 2), such as HYDRUS-1D (Rivera Villarreyes et al., 2014) and JULES (Iwema et al., 2017; Peng, Tanguy, et al., 2021), simulate the movement and retention of water in soil using hydrological equations like Richards' equation (Richards, 1931). These models provide a detailed and interpretable picture of SWC dynamics that could be used as reference for harmonizing SWC observations. However, these models require extensive inputs, such as soil texture, boundary conditions, and meteorological forcing, and are sensitive to parameter uncertainty. Thus, their value lies in high-resolution simulation, though their complexity and reliance on input assumptions limit their applicability for harmonizing multiple, independent SWC products within the framework considered in this study.

Based on the review, harmonization was structured into four components of increasing complexity: unit, temporal,

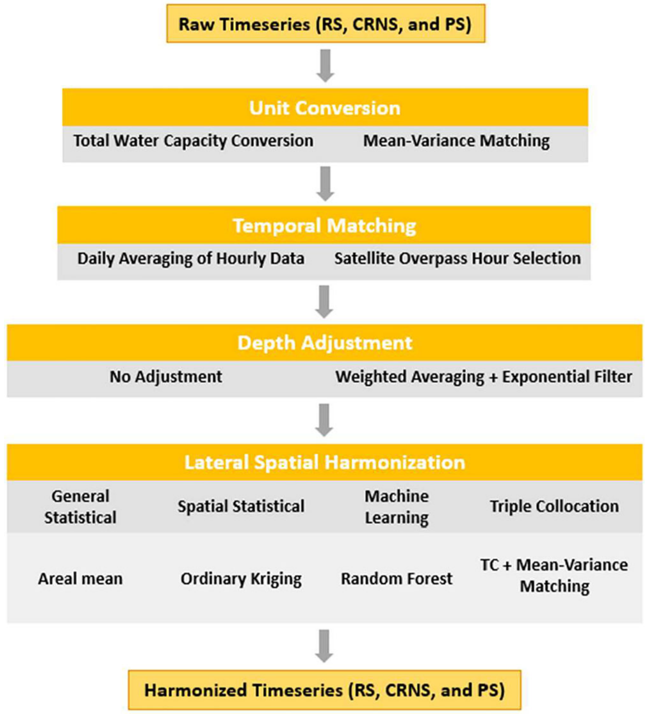

FIGURE 3 Workflow of the harmonization process for remote sensing (RS), cosmic-ray neutron sensing (CRNS), and point-scale (PS) soil water content (SWC) time series. The process includes four main steps: unit conversion, temporal matching, depth adjustment, and lateral spatial harmonization, each with two or more method options. The final outputs are harmonized time series across all sensor types. TC, triple collocation.

vertical (depth), and lateral spatial. To facilitate a comparative analysis, the two most used methods were selected for each of the first three components (Figure 3). Given its greater complexity and prevalence in the literature, lateral spatial harmonization required a broader set of approaches. For this component, a single representative method was chosen from each category outlined in Figure 2. However, process-based models were excluded since these models produce entirely synthetic time series, rather than the three distinct outputs from PS, CRNS, and RS (Figure 3). Four principles guide the selection of harmonization methods:

1. Minimizing reliance on field measurements, ensuring applicability in regions where in situ data collection is challenging.
2. Avoiding synthetic data generation, as the study aims to work with real observations rather than model-generated estimates.
3. Preserving the intrinsic nature of each dataset, preventing excessive transformation that would artificially align datasets rather than make them more comparable.
4. Avoiding data fusion, maintaining harmonization as a distinct preprocessing step.

The chosen methods and their implementation are described in the subsequent sections.

Before applying harmonization methods, a QC step was performed on all three datasets to remove obvious outliers that could distort later analyses, particularly those relying on minimum and maximum values (e.g., in unit harmonization). For PS and CRNS data, values exceeding 0.6 m^3/m^3, following the guidelines proposed by W. A. Dorigo et al. (2013), or equal to zero, were excluded. For the RS product, the same filtering was applied after converting saturation values to VWC. This simple yet necessary step ensured that physically unrealistic values did not affect threshold-based or statistical calculations while remaining within the scope of a minimal preprocessing workflow.

2.4 | Unit harmonization

In this study, SWC from PS and CRNS is expressed in VWC, while the RS product is expressed in relative saturation. To enable intercomparison and harmonization across datasets, a unit transformation of the RS product into VWC was required. Two widely used families of methods have been identified in the literature:

1. Soil physics-based scaling methods, for example, van Genuchten (1980), which convert saturation into VWC using soil physical limits between a minimum water content θ_{min} and a maximum water content θ_{max} (Equation 3). In most formulations, saturation is assumed to reach porosity (ϕ) under fully saturated conditions, while the residual water content defines the lower bound (van Genuchten, 1980). Alternative definitions exist, for example, WP or the minimum of a ground-based time series as θ_{min} (Qiu et al., 2024; Schmidt et al., 2024).
2. Statistical bias-correction methods (Reichle & Koster, 2004), which adjust the RS distribution to match ground data. These include mean-variance matching (Bauer-Marschallinger et al., 2019; Massari et al., 2015), linear regression, and cumulative distribution function (CDF) matching (Crow et al., 2012; Massari et al., 2015). Such methods do not require soil input data, but they alter both the mean and variance of RS data, potentially reducing the preservation of natural RS dynamics. Longer ground data records improve the robustness of the estimated statistical parameters.

To represent both families, one method was selected from each group (Table 2):

1. Total water storage capacity scaling (Equation 4), where ϕ was derived from BD using SoilGrid's data and Equation (5) (Saxton & Rawls, 2006). The θ_{min} was considered as the residual water content (extracted from PTFs) or, if lower, the lowest hourly ground observation, while the maximum was set either to porosity or, if higher, to the maximum ground observation to ensure physical plausibility. Re-emphasizing the necessity of QC; without it, the min and max values are often dominated by outliers.

$$\mathrm{SWC} = S \cdot \left(\theta_{\mathrm{max}} - \theta_{\mathrm{min}}\right) + \theta_{\mathrm{min}} \tag{4}$$

$$\phi = 1 - \frac{\mathrm{BD}}{2.65} \tag{5}$$

Here, 2.65 g/cm^3 represents the average particle density of mineral soils (Saxton & Rawls, 2006). This method is physically interpretable and preserves the RS product's natural variability but is sensitive to uncertainties in BD and ϕ maps, which are often coarse (Minasny & McBratney, 2016). A longer time series of ground data improves the reliability of the extrema used in this approach.

2. Variance matching, which rescales RS values to align with the mean (μ) and standard deviation (σ) of the ground dataset:

$$\mathrm{SWC} = \mu_g + \left(\frac{\sigma_g}{\sigma_{\mathrm{RS}}}\right) \cdot \left(S - \mu_{\mathrm{RS}}\right) \tag{6}$$

where μ_g and σ_g are the mean and standard deviation of the ground data (PS or CRNS), and μ_{RS} and σ_{RS} are the corresponding values from the RS dataset. This approach is broadly applicable but modifies the original RS variability and reduces physical interpretability.

Each method was applied twice, once using PS and once using CRNS as the reference dataset, resulting in four harmonized RS versions. These harmonized products were then evaluated against the remaining ground-based dataset using statistical metrics enabling both cross-method and cross-reference analysis. For plausibility testing within FC and WP, a depth of 0–5 cm was assumed for the RS product's initial depth assumption. To ensure consistency, the PS sensor located nearest to each CRNS station was selected for this step's analysis.

2.5 | Temporal resolution harmonization

In this study, PS and CRNS sensors provide sub-daily (hourly) data, while the RS product offers daily estimates. This mismatch in temporal resolution requires careful alignment to ensure meaningful comparisons and analysis, especially considering that, although the RS product is provided daily, most satellite missions, such as SMAP (Entekhabi et al., 2010), have revisit cycles of several days, depending on orbit geometry and regional coverage. In general, three main

TABLE 2 A summary of the qualitative differences between the two unit conversion methods.

Method	Scaling	Bias removal	Preservation of RS dynamics	Strengths	Weaknesses
Total water capacity conversion	Yes (within soil range)	Partial (implicit via scaling)	High	Physically meaningful, retains original signal	Dependent on soil inputs; coarse BD/φ data may limit accuracy
Mean-variance matching	Yes (statistical)	Yes (explicit mean correction)	Moderate to low	Statistically aligned with ground data	Alters RS variance and mean; reduced physical interpretability

Abbreviations: BD, bulk density; RS, remote sensing.

TABLE 3 A summary of the qualitative differences between the two temporal harmonization methods.

Method	Data use efficiency	Synthetic data	Preservation of dynamics	Suitability	Weaknesses
Daily averaging of hourly data	High	No	Moderate	Climate studies, long-term monitoring	Smooths out short-term variations, especially events
Satellite overpass hour selection	Low	No	High (specific timestamps)	Sensor-to-sensor alignment, validation use	Ignores full daily cycle, reduced statistical power

strategies have been identified in the literature for temporal harmonization:

1. Aggregation of high-frequency data to match the lower-frequency product (Wang et al., 2021).
2. Selective sampling of hourly data based on satellite overpass times (Bauer-Marschallinger et al., 2019).
3. Disaggregation of daily or multi-day RS data to higher-frequency time steps using interpolation or modeling techniques (Fang et al., 2018).

The first approach, aggregation, is straightforward and retains all original ground observations, smoothing them into a single representative daily value. This is useful for applications like water balance studies (Pauwels et al., 2001) or trend analysis (W. Dorigo et al., 2012), where sub-daily variability is less critical. The second approach focuses on temporal alignment by extracting ground data from the same hours as the satellite passes. While this enables strict point-to-point comparison, it sacrifices information from the rest of the day and may miss important diurnal soil moisture changes. The third approach, disaggregation, introduces synthetic values and contradicts the key assumption stated in the introduction, namely, that harmonization should not rely on artificial data generation. Furthermore, temporal downscaling, without detailed meteorological inputs like precipitation or irrigation, would add another layer of uncertainty. For these reasons, this approach was excluded from our analysis. Therefore, two temporal harmonization methods were selected for implementation (Table 3):

1. Daily averaging of PS and CRNS hourly data to match the RS time step.
2. Selection of PS and CRNS hourly values corresponding to Sentinel-1 overpass times: 05:00 and 17:00 UTC for Italian sites and Nucice, and 06:00 and 18:00 UTC for UK sites.

For statistical evaluation, each harmonized ground dataset (using the two temporal approaches) was compared with the RS product that had been previously converted to VWC using the alternate ground source. FC and WP specific to PS (0–5 cm) and CRNS (0–30 cm), based on a preliminary consideration of their depth range, were used to enable plausible analysis for the temporal component. Since one PS from each site was needed for analysis of this step, the sensor closest to the CRNS was chosen. SWC is typically slow changing over short periods due to its "memory" (Rahmati et al., 2024), a lag in response to external forcing like rainfall or evapotranspiration. Literature suggests this memory can persist for several months in deeper soil layers or integrated SWC states, whereas memory in surface soil layers is typically much shorter (D. Liu et al., 2014; Rahmati et al., 2024; Shinoda & Nandintsetseg, 2011), which supports daily analysis for many hydrological applications. However, short-term processes such as irrigation or heavy rainfall may produce rapid fluctuations better captured at the hourly scale (Baroni & Oswald, 2015). Selecting the appropriate time resolution depends on the trade-off between capturing dynamic variability and ensuring dataset consistency.

2.6 | Soil depth harmonization

SWC varies not only across space and time but also with depth. This vertical heterogeneity arises from complex interactions between soil structure, water infiltration, evaporation,

TABLE 4 A summary of the qualitative differences between the two depth harmonization approaches.

Method	Adjustment type	Synthetic output	Data needed	Strengths	Weaknesses
No adjustment	None	No	None	Preserves original data; simple; reflects practical use	Ignores physical vertical mismatch; less precise
Weighted averaging or exponential filter	Physically and empirically based	Partially (RS)	PS weights, optimized T	More realistic vertical representation; flexible for CRNS alignment	Requires tuning; weights depend on soil/vegetation inputs

Abbreviations: CRNS, cosmic-ray neutron sensing; RS, remote sensing.

and root water uptake (Delval et al., 2025; Kuhlmann et al., 2012). In SWC measurement, each sensing technique observes water content at different vertical ranges. RS typically captures the top few centimeters (Entekhabi et al., 2010), and PS sensors are often installed at specific depths, while CRNS integrates moisture over a deeper and broader vertical domain. This creates a scale mismatch in the depth dimension, making direct comparisons between datasets challenging, particularly between RS/CRNS and PS/CRNS pairs. Although the average penetration depth of CRNS is often reported as spanning from 10 to 50 cm, studies show that its sensitivity is highest near the surface and decreases exponentially with depth (Franz et al., 2012; Köhli et al., 2015; Zreda et al., 2008). This means that the topsoil contributes most significantly to the CRNS signal, justifying a certain level of comparability with RS and shallow PS sensors, as done by (Colliander et al., 2017). However, for a more accurate and physically grounded harmonization, especially when datasets differ in vertical sensitivity or sampling depth, dedicated methods are required.

In the conducted literature review, the following methods have been identified:

1. The exponential filter introduced by Wagner et al. (1999), and the recursive form of that (Albergel et al., 2008) emerged as the most used methods for RS vertical adjustment.
2. Statistical matching (Reichle & Koster, 2004; N. Zhang, Quiring, et al., 2017).
3. ML methods (J. Li & Zhang, 2021).
4. Process-based modeling (e.g., HYDRUS-1D [Rivera Villarreyes et al., 2014; Scheiffele et al., 2025]).

Most of these alternatives either rely on extensive auxiliary data (e.g., hydraulic parameters and meteorological inputs) or generate synthetic time series that conflict with the goal of preserving the intrinsic characteristics of the original datasets. Additionally, applying such methods in the vertical dimension may introduce compounded effects when followed by further transformations in the lateral spatial harmonization step. In this study, two harmonization strategies were employed to address vertical scale mismatches (Table 4):

1. *No adjustment (direct comparison)*: In this approach, RS, PS, and CRNS datasets are directly compared without modifying their depth of representation. This decision is supported by two key arguments. First, RS and PS (the shallowest depth, mainly 5 cm) sensors in this study both focus on near-surface soil (around 0–5 cm), while CRNS, though deeper in theory, is more sensitive to upper layers, especially under wet conditions. Second, for many practical applications, including drought monitoring and irrigation scheduling, root-zone SWC is often most relevant, while near-surface SWC remains important for surface-oriented processes and rapid hydrological responses (Entekhabi et al., 1996; Seneviratne et al., 2010). Moreover, avoiding transformation prevents the introduction of touched time series and preserves the intrinsic variability of each dataset. Nonetheless, this approach simplifies the vertical structure of the soil and may not fully reflect the physical differences among sensor types.
2. *Weighted averaging and exponential filtering*: This method attempts a more physically meaningful alignment by adjusting PS and RS datasets to approximate the undefined depth sensitivity of CRNS.

(a) PS adjustment via weighted averaging: When multiple PS sensors were available at different depths, a weighted depth-averaged SWC value was computed, with the revised depth weighting scheme designed to approximate the SWC signal sensed by CRNS (Schrön et al., 2017). This formulation (Equation 7) provides improved estimates compared to earlier linear weighting schemes, such as Franz et al. (2012), by accounting for neutron physics and environmental factors. The weights were obtained using the authors' publicly available Excel tool, with site-specific parameters.

$$W_d\left(r,\ \mathrm{SWC}, p, H_{\mathrm{veg}}\right) = e^{-2/D} \tag{7}$$

In Equation (7), W_d represents the vertical weighting function applied to PS measurements at the depth d, accounting for the CRNS sensitivity profile. The effective penetration D (Köhli et al., 2015) depends on the horizontal distance from the sensor r, SWC itself, air pressure p, and vegetation height H_{veg}. This formulation captures the physics of neutron attenuation and allows deeper measurements to be weighted appropriately when comparing with CRNS observations.

(b) *RS adjustment via exponential filter:* To align RS observations with the broader CRNS depth sensitivity, an exponential filter was applied as described by Wagner et al. (1999). The filter smooths the RS time series while simulating moisture propagation to deeper layers:

$$\theta_{\mathrm{filt}}\ (t) = \theta_{\mathrm{filt}}\ (t-1) + K\ .\ \left(\theta\ (t) - \theta_{\mathrm{filt}}\ (t-1)\right) \quad (8)$$

where $\theta_{\mathrm{filt}}\ (t)$ is the filtered RS at time t, $\theta\ (t)$ is the original RS observation, $K = \frac{1}{1+T}$, and T is the characteristic time length. The T values tested ranged from 1 to 30. The optimal value for each site was selected based on R and ubRMSD between the filtered RS signal and the PS/CRNS datasets. This method adjusts RS data without producing fully synthetic series, preserving the core behavior of the RS product while approximating deeper dynamics. However, it introduces two key limitations: first, there is a risk of overfitting, as optimizing T may inadvertently fit site-specific noise rather than true vertical response, especially when data records are short or noisy; and second, the filter reduces high-frequency variability, potentially obscuring rapid moisture changes due to rainfall or irrigation. Additionally, because the method does not use explicit soil physical properties, it remains an empirical approximation of vertical behavior.

Statistical metrics were computed using CRNS as the reference, since its values remained unchanged. The same depth ranges used for unit and temporal harmonization across the three sensors were applied in the plausible analysis (using FC and WP), and also the single PS chosen for each site was the nearest to the CRNS.

2.7 | Harmonization of lateral spatial variability

When examining the issue of harmonizing datasets with different spatial footprints, two general methodological schools of thought can be identified. The first involves statistical and geostatistical models, which reconcile differences through mathematical relationships. Geostatistical models offer a more meaningful alternative to simple statistical techniques because they incorporate spatial structure and variability into the analysis. The second approach is more conceptual or physically informed. It attempts to explain and quantify SWC variability by considering environmental drivers like vegetation, soil type, topography, and land use (Brocca et al., 2010; Emamalizadeh et al., 2024; Gibon et al., 2024; Vereecken et al., 2008). Although this approach aligns closely with the physical processes behind SWC dynamics, it lacks standardized indices and widely adopted formulas, limiting its current use in harmonization workflows. While we acknowledge the value of these physically informed methods, their implementation requires site-specific knowledge and detailed environmental data. As such, dedicated research studies on that topic are needed. This study, therefore, focuses on the first approach, methods grounded in statistical and spatial statistical techniques, because they are currently more accessible and broadly used in the literature.

The areal average was selected from general statistical methods due to its simplicity and common use in the literature, as seen in studies from our review (Heathman, Cosh, Merwade, et al., 2012; Jacobs et al., 2004; Robinson et al., 2008). Based on the concept of temporal stability (Vachaud et al., 1985), several studies, such as Albergel et al. (2012), Brocca et al. (2010), and Gruber et al. (2013), have shown that PS measurements may, under certain conditions, represent coarser-scale averages like those from CRNS or RS. In this method, CRNS and RS are not used as inputs, and only PS values are averaged across the relevant area. More representative results would be achieved when multiple PS sensors are spatially distributed within the CRNS footprint or RS pixel. For all lateral spatial categories, the plausibility-based analysis described in Section 2.2 was conducted using a common 0- to 30-cm soil depth range across all sensors. This choice reflects the outcome of the preceding vertical harmonization step, in which the resulting SWC time series represent an integrated soil layer rather than a specific measurement depth. The plausibility analysis evaluated harmonization performance by quantifying changes (Δ) in the number of observations falling within predefined SWC thresholds (i.e., FC and WP) before and after applying each harmonization method. Additionally, statistical performance metrics were computed based on the sensor time series that were modified by each lateral harmonization approach. Depending on the method, some datasets may remain unchanged. For example, in areal averaging approaches, PS observations are aggregated and serve as the benchmark, while changes are assessed for CRNS and RS products relative to the PS-derived reference.

For spatial statistical methods, ordinary kriging was used because it is simple, widely used, and makes use of the spatial pattern of the data without needing extra predictors. It gives reliable estimates when there are enough sensors, but it needs a good number and spread of points to work well (Wackernagel, 2003). Since most of our sites do not meet a sufficiently large number of spatially distributed observation points for reliable variogram estimation, we applied this method only at Bondeno (eight sensors) and Marquadt (30 sensors). At the Bondeno site and, to a lesser extent, the Marquardt site, the limited number of observation points still restricts robust variogram estimation. As a result, kriging-based harmonization at these sites should be interpreted cautiously and primarily as an exploratory comparison rather than a definitive spatial interpolation. For these two sites,

TABLE 5 Overview of lateral spatial harmonization methods with key features, strengths, and limitations to support method selection.

Category	Example methods	Statistical or physical	Spatial awareness	PS sensors needed	Ease of implementation	Strengths	Limitations
General Statistics	OLS, Ridge Regression, and Arithmetic Mean	Statistical	Low	1 or more	Easy	Simple, fast, low data needs	Assumes linearity, limited spatial adaptation
Spatial Statistics	Kriging, Variogram analysis	Statistical	High	Several	Moderate	Honors spatial autocorrelation, well-suited for mapping	Needs a dense PS network, sensitive to spatial assumptions
Machine learning	RF, kNN, SVM, NN	Statistical	Medium	Several	Moderate to difficult	Captures nonlinearity, handles large variability	Data-hungry, opaque, may shift SWC patterns
Triple collocation (TC)	Standard TC, Extended TC (Yuan et al., 2020)	Statistical	Low	1 or more	Moderate	Error decomposition without a reference	Requires 3 datasets, dependent on assumption validity
Process-Based Models	HYDRUS-1D, JULES	Physical	Medium to high	Not needed	Difficult	Physically meaningful, rich simulation capability	Data-intensive, parameter uncertainty, and computational cost

Abbreviations: kNN, k-Nearest Neighbors; NN, neural networks; OLS, ordinary least squares; PS, point-scale; SVM, support vector machines; SWC, soil water content.

ordinary kriging was used to estimate SWC within the CRNS and RS footprints based on the PS sensors located inside each footprint. The variogram model used for ordinary kriging was spherical. Consistent with previous studies on SWC from PS, the empirical variograms exhibited strong nugget effects and short correlation ranges, reflecting pronounced small-scale variability and measurement noise.

Considering ML techniques, RF was chosen due to its simplicity, reduced risk of overfitting compared to other ML models, and widespread use in the literature (Belgiu & Drăgu, 2016; Breiman, 2001). It was applied for both upscaling and downscaling around the CRNS footprint. For upscaling, PS sensors located within the CRNS footprint were first aggregated using distance-based weighting to derive a representative PS-based SWC estimate at the CRNS scale. This aggregated PS estimate was then used within the RF framework to model the relationship between PS-derived and CRNS-scale SWC, rather than applying RF directly to individual PS measurements. For downscaling, RS data served as the main predictor, with PS sensors inside the RS pixel used as the other predictors, also weighted by distance. RF's ability to model nonlinear relationships (Table 5) and its robustness to multicollinearity make it suitable for this task, though it still requires a reasonably dense PS network and does not directly account for physical processes.

For TC-related approaches, as explained before, after identifying the lowest error dataset using TC, harmonization can proceed using simpler methods like mean-variance matching (Equation 6), as done in our study. This method adjusted other datasets to match the reference dataset's (lowest variance error) mean and standard deviation. It was opted against more complex transformations, such as CDF matching (L. Zhu et al., 2023), to preserve the original distribution shape and avoid overfitting.

3 | RESULTS AND DISCUSSION

3.1 | Unit harmonization

Regarding performance metrics, the mean R for six sites remained consistent across both methods, which is expected given that both approaches incorporate scaling in their formulations. However, the ubRMSD showed slight differences. When using CRNS and PS as reference sensors, Method 1 (total water capacity conversion) exhibited delta ubRMSD (difference of ubRMSD before and after applying harmonization methods) values of −0.12 and −0.14, respectively, while Method 2 (mean-variance matching) showed slightly higher delta values of −0.16 and −0.18. This marginal increase in delta ubRMSD for Method 2 is linked to its statistical shifting mechanism, which improves the overall closeness of dataset means.

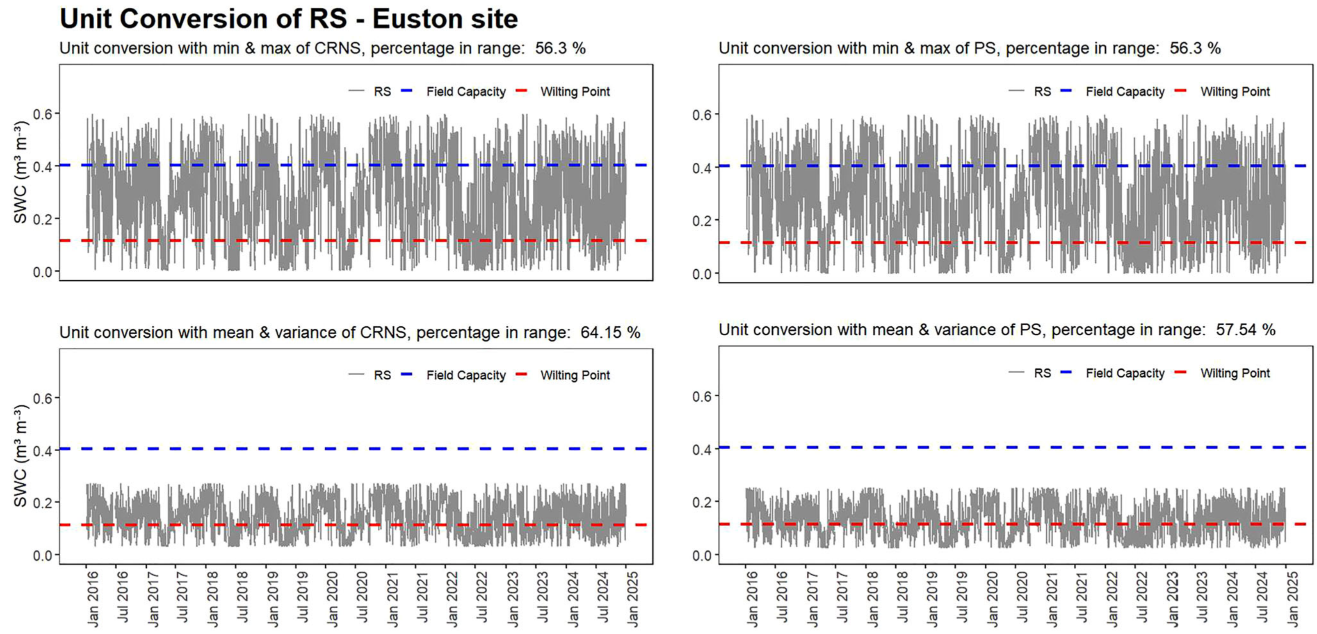

FIGURE 4 Unit conversion of remote sensing (RS) time series (gray line) at the Euston site using two methods: Total water capacity conversion (top row) and mean-variance matching (bottom row) with cosmic-ray neutron sensing (CRNS) (left column) and point-scale (PS) (right column) as reference datasets. Dashed lines indicate field capacity (FC) (blue) and wilting point (WP) (red); percentage values show the proportion of RS data falling within this range after conversion at the Euston site. SWC, soil water content.

The percentage change in RS points falling between the WP and FC thresholds of the RS 0–5 cm layer, before and after unit harmonization, was also evaluated. Method 1 demonstrated a moderately higher percentage, with 37% and 36% of RS points falling within the thresholds considering CRNS and PS as ground sensors, respectively. In contrast, Method 2 yielded lower plausibility results of 35% and 29%. This reduced performance in Method 2 is attributed to its high scaling of the RS time series, which diminishes the inherent variability of the RS data, often causing a significant portion of points to fall below the WP, as illustrated in Figure 4 for the Euston site as an example.

Considering these quantitative and qualitative (Table 2) observations, Method 1 is preferred for unit harmonization, and the RS data converted using Method 1 with CRNS data will serve as the input for the next harmonization step.

3.2 | Harmonization for temporal resolution

Across six sites, performance metrics showed no significant differences between the two methods. As an example, the results for the Euston site are presented in Figure 5. The change in plausibility check of ground values within their WP–FC ranges using Method 1 (satellite overpass hour selection) was nearly 0% for CRNS and 16% for PS. Using Method 2 (daily average of hourly values), the results were similar, almost 0% for CRNS and 16% for PS. The findings suggest that the method used to select the SWC data, either from a specific satellite overpass time or as a daily average, has a negligible impact on the overall results. To be clarified further, both preserve the key statistical properties of ground data equally well. This is because SWC typically changes slowly over short periods due to its “memory,” a lagged response to external factors like rainfall or evapotranspiration. This stability is a key finding, as it validates the use of a single daily measurement for certain applications, simplifying data collection and analysis. SWC’s slow response is also influenced by soil type, with finer textured soils like clay having a higher water-holding capacity and thus a longer “memory” than sandy soils. This means that a single day’s worth of data from a given location, whether represented by an average or a specific time of day, will likely have a similar overall value. This similarity allows users to choose either approach based on their particular application (Table 3). This consistency is particularly valuable for large-scale studies where collecting a single daily snapshot is more practical than continuous monitoring, providing flexibility in data acquisition without sacrificing accuracy. In this study, to account for the full diurnal variability, Method 2 was selected, which will serve as input for the next harmonization steps.

3.3 | Depth harmonization

On average across the seven sites, while PS metrics remained essentially unchanged, RS showed a notable improvement, with $\Delta R = 0.15$ and ΔubRMSD $= -0.03$, confirming that

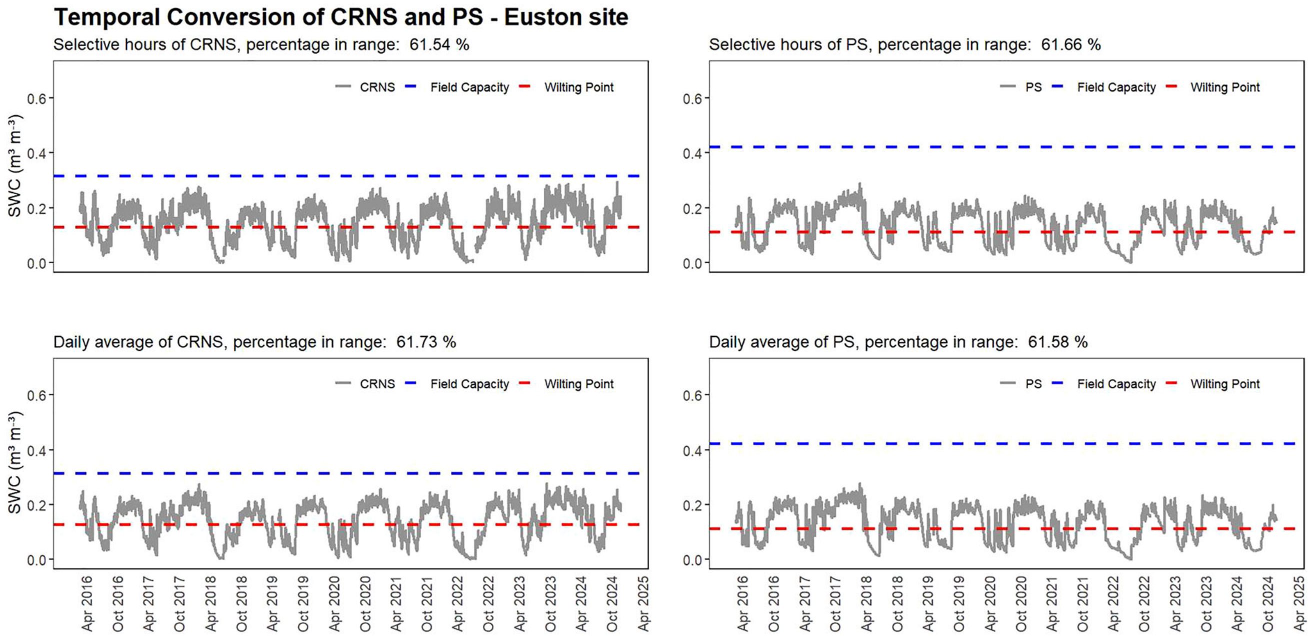

FIGURE 5 Temporal conversion of cosmic-ray neutron sensing (CRNS) (left column, gray line) and point-scale (PS) (right column, gray line) soil water content (SWC) at the Euston site using two methods: selective hours corresponding to satellite overpass times (top row) and daily averages of all hourly values (bottom row). Both methods show similar percentages of values within the range between wilting point (WP) (red dashed line) and field capacity (FC) (blue dashed line), with minimal impact on the temporal structure of the data.

the filtered RS series better captures the temporal patterns observed in the CRNS data. The change in the plausibility of values within the WP–FC range after applying depth harmonization was negligible for PS (≈0%) and around 12% for RS. Two algorithms were used for the second method: a weighted average for PS and an exponential filter for RS. The choice of these algorithms reflects the different nature of the measurements: PS data, already relatively stable and local, benefit from a simple weighting across depths, while RS data, which often contain high-frequency variability unrelated to soil processes, require stronger temporal smoothing.

As shown in Figure 6 (Euston example), the exponential filter effectively reduces spurious short-term fluctuations in the RS time series, improving its alignment with ground-based measurements. This harmonization step is particularly important for C-band SAR SWC data, which are generally more prone to noise than L-band products due to their shallow sensing depth and sensitivity to surface roughness and vegetation.

The qualitative comparison (Table 4) also highlights key advantages of Method 2 over Method 1 (no adjustment). By harmonizing RS, PS, and CRNS to a consistent effective depth (a range rather than a single value), Method 2 provides a more physically meaningful basis for cross-comparison and subsequent integration. This ensures that the three observation types can be treated on equal footing, reducing depth-related biases in later analyses. The approach relies on a site-specific characteristic time length (T), with an average of approximately 6 days across all sites. This parameter reflects the typical SWC "memory," that is, the time required for the soil profile to equilibrate after a rainfall or drying event and is therefore critical for aligning RS with the dynamics captured by CRNS sensor.

Figure 7 further illustrates how performance metrics vary with different T values at the Euston site as an example, showing that overly short T values under-smooth the RS signal, while excessively long T values risk removing meaningful variability. This sensitivity analysis demonstrates that calibrating the filter strength on a site-specific basis can improve performance under heterogeneous conditions, although previous studies have shown that a single characteristic time length may be sufficient for some applications (Albergel et al., 2008; Ford et al., 2014). For these reasons, Method 2 is preferred, as it balances physical realism with statistical performance, and its output will be used in the next spatial harmonization step.

3.4 | Lateral spatial harmonization

Using the areal mean from the general statistical category, statistical analysis revealed that the mean ubRMSD of seven sites decreased by −0.03 for CRNS and −0.07 for RS, indicating reduced divergence between the harmonized estimates and reference data. Additionally, the mean R increased substantially, by 0.48 for RS and 0.17 for CRNS, suggesting stronger

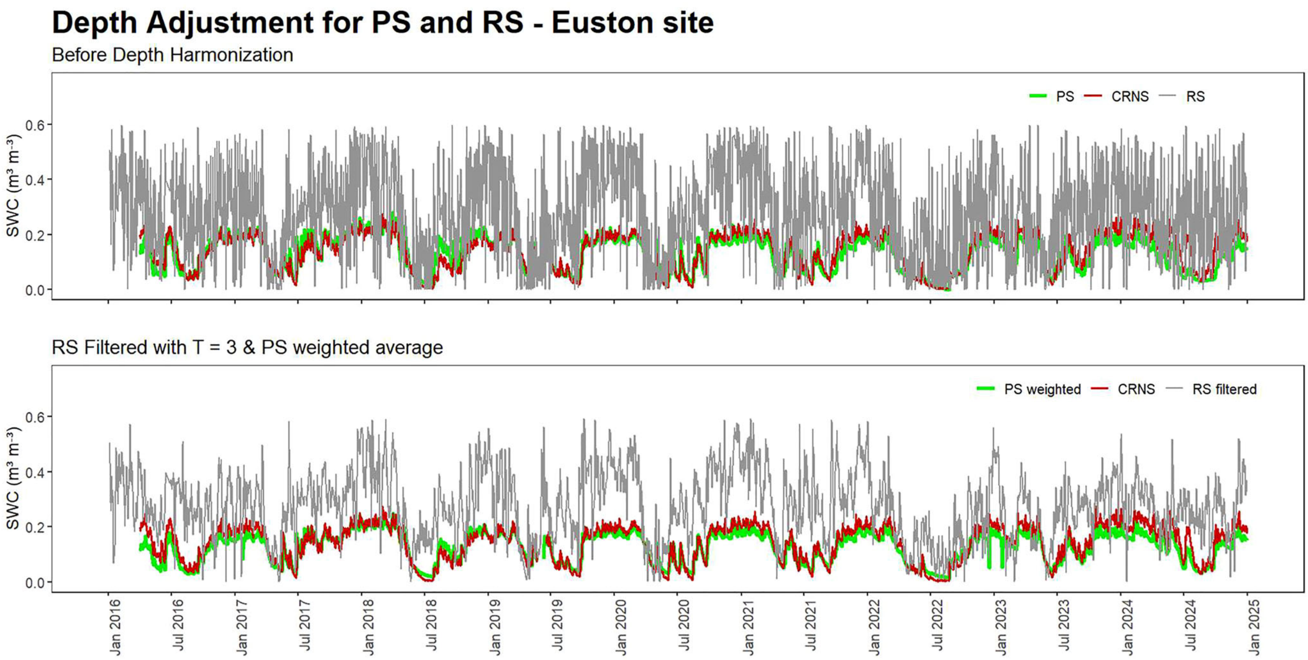

FIGURE 6 Depth adjustment of point-scale (PS) and remote sensing (RS) at the Euston site. The top panel shows the original time series before harmonization. The bottom panel illustrates the effect of applying a weighted average to PS and an exponential filter to RS with a site-specific time length of $T = 3$ days. CRNS, cosmic-ray neutron sensing; SWC, soil water content.

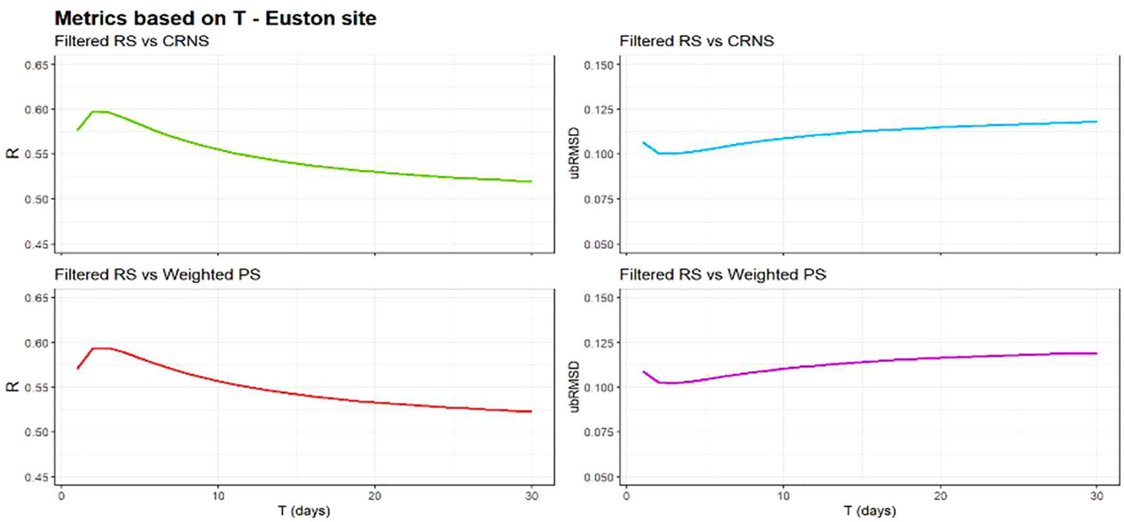

FIGURE 7 Effect of T on R (left column) and unbiased root mean square deviation (ubRMSD) (right column) between filtered remote sensing (RS) and ground observations (cosmic-ray neutron sensing [CRNS] and weighted point-scale [PS]) at the Euston site. Optimal performance is observed around $T = 3$ days, with higher T values leading to reduced correlation and increased ubRMSD. SWC, soil water content.

agreement post-harmonization. However, this improvement primarily stems from both CRNS and RS estimates now being derived from PS values, effectively replacing their original signals rather than reconciling them.

The plausibility variation before and after spatial harmonization, calculated using the areal mean of PS sensors' data to estimate SWC within CRNS and RS footprints, showed notable differences between the two methods. On average, the areal mean method led to an approximately −6% change in the number of CRNS observations falling within the defined plausibility thresholds, while the impact on RS observations was negligible (close to zero). Although this approach is theoretically feasible even with a single PS sensor, its performance varied significantly across study sites. Most locations

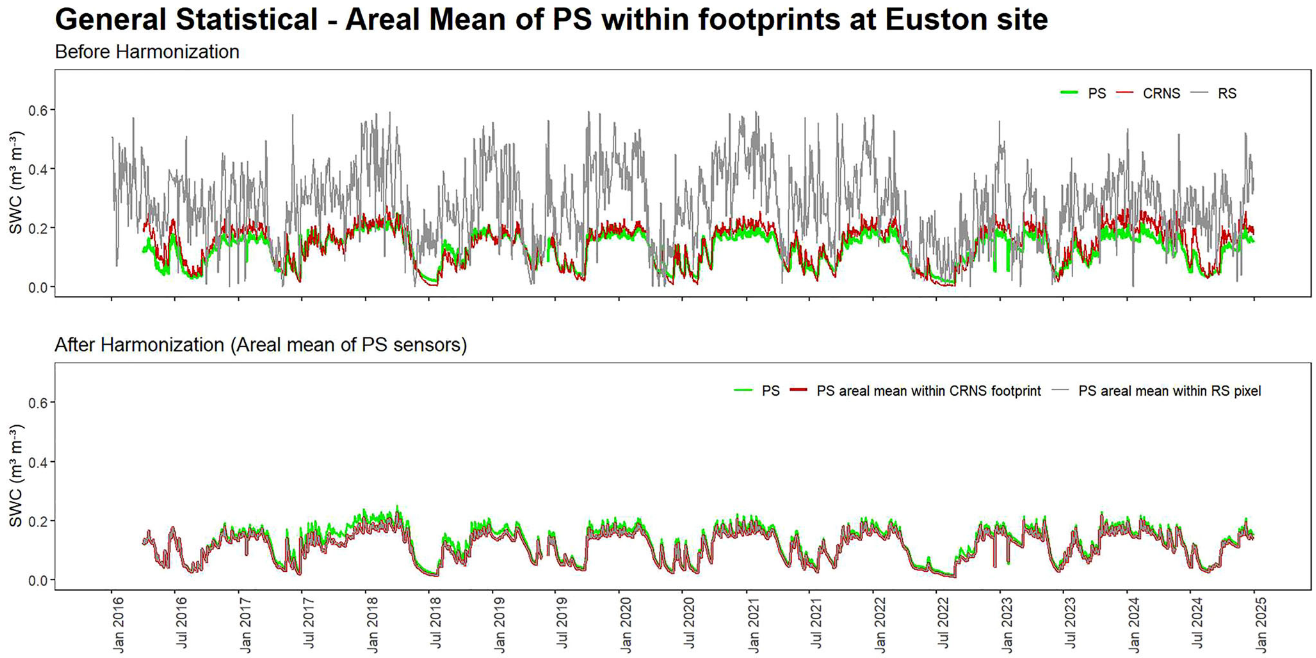

FIGURE 8 Lateral spatial harmonization at the Euston site using the areal mean of point-scale (PS) sensors within cosmic-ray neutron sensing (CRNS) and remote sensing (RS) footprints. The top panel shows the original time series before harmonization, while the bottom panel presents newly produced CRNS and RS estimates derived from PS areal averages. SWC, soil water content.

exhibited strongly negative percentage changes, likely due to spatial heterogeneity or discrepancies in scale representation. However, the Marquadt site, which features a denser PS network, counterbalanced these effects (e.g., 80% increase of plausibility check for RS), resulting in a more stable overall outcome. This underscores the importance of a well-distributed and sufficiently dense PS network to improve the reliability of spatial harmonization.

As shown in Figure 8 for the Euston site example, this harmonization approach does not directly use the original RS or CRNS time series as inputs. Instead, PS observations are used to generate two separate SWC time series: one representing the CRNS footprint and one representing the RS footprint. Because both series are derived from the same underlying PS measurements, the resulting harmonized time series closely match each other. While this demonstrates that the method enforces consistency, it also means that unique scale-dependent information from CRNS and RS is lost, as the harmonized output predominantly reflects the PS-based areal mean. This trade-off highlights a key limitation: the approach prioritizes uniformity over preserving the distinct characteristics of each sensor's native measurements.

Using the second lateral spatial harmonization approach, a geostatistical approach was implemented by applying ordinary kriging to the PS network to estimate mean SWC values representative of the CRNS and RS footprints. Due to its reliance on a sufficiently dense and spatially distributed set of PS sensors, only two of the seven study sites (Bondeno and Marquadt) met the minimum requirements for this method. At these sites, the improvements were substantial: performance metrics also confirmed the increases, with correlation R enlarged by 0.43 for CRNS and 0.44 for RS, alongside reductions in ubRMSD of −0.04 and −0.05, respectively. The proportion of values within the WP-FC thresholds increased by 16% for CRNS and 30% for RS. These gains are considerably higher than those obtained with simpler statistical approaches, underscoring the advantage of explicitly modeling spatial variability.

However, as illustrated in Figure 9 for the Bondeno site, the method is not without limitations. Because kriging predictions are based solely on PS observations, the resulting synthetic CRNS and RS series closely mirror PS dynamics, reducing the distinctiveness of each sensor type. In addition, the relatively short PS time series at these sites constrained the temporal overlap with CRNS and RS, leading to a reduction in data availability after harmonization. These factors highlight the importance of both sensor density and record length when applying kriging for harmonization purposes.

The quantitative improvements observed suggest that kriging can be an effective harmonization tool under suitable conditions. It preserves spatial structure reasonably well and provides statistically grounded estimates, which may be useful for applications like irrigation planning or localized hydrological modeling. However, its performance depends heavily on the density and distribution of PS sensor data. Expanding PS networks, particularly in areas with high soil or land cover variability, could improve the method's reliability across more diverse sites.

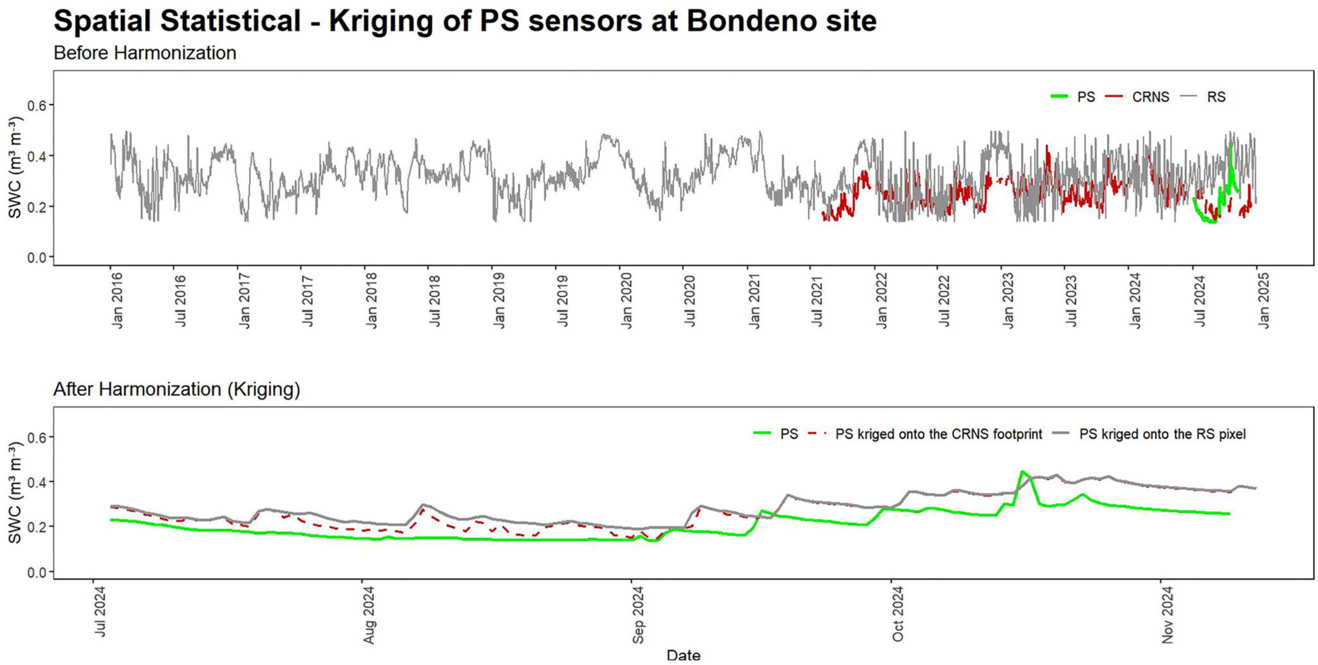

FIGURE 9 Soil water content (SWC) time series at the Bondeno site before (top) and after (bottom) spatial harmonization using ordinary kriging of point-scale (PS) data to estimate mean values within cosmic-ray neutron sensing (CRNS) and remote sensing (RS) footprints.

RF, a widely used ML method, was implemented to address the lateral spatial harmonization challenge by upscaling PS data and downscaling RS data to the intermediate CRNS footprint. For upscaling, PS measurements within the CRNS radius were used as inputs, with their contribution weighted according to distance from the CRNS sensor. This allowed the model to account for local heterogeneity while producing a synthetic estimate at the CRNS scale. For downscaling, RS values were employed as the primary predictor, supported by in situ PS as the other predictors. In both cases, the model was trained against observed CRNS SWC, thereby aligning the predictions to the CRNS footprint.

Statistical metrics showed notable improvements: ubRMSD decreased by −0.03 for PS and −0.08 for RS, while *R* increased substantially, by 0.19 for PS and 0.54 for RS. These values indicate that RF was particularly effective in reducing random discrepancies and improving dynamic agreement, especially for RS, which originally exhibited the weakest alignment with CRNS. The performance evaluation revealed that the mean difference between original and RF-modeled CRNS SWC was negative (−3% using PS and −10% using RS), both within the CRNS thresholds. To be explained more, most sites showed a slightly positive change in the plausibility check; however, the Italian sites, with markedly negative percentage changes (around −30% for Bondeno and −45% for Imola), pulled the overall average into negative values.

However, visual inspection of the harmonized series (Figure 10) revealed that the modeled CRNS closely tracks the original CRNS time series, often reproducing its dynamics with minimal deviation. While this suggests high predictive skill, it also raises concerns of overfitting. In practice, RF may have captured site-specific patterns too precisely, limiting the method's generalizability across sites or periods. This blurs the line between harmonization and data fusion: rather than preserving the independent characteristics of PS and RS, RF effectively forces them into the CRNS signal domain.

In the final method, in which the sensor with the lowest error variance is first identified through TC and the remaining datasets are subsequently scaled to match its mean and variance, distinct impacts across the three sensor types were observed.

As theoretically expected, the *R* remained unaffected by this rescaling procedure, since the method does not alter temporal co-variability. However, improvements were visible in terms of error metrics: the ubRMSD decreased by −0.02 for PS and −0.04 for RS, indicating a modest yet consistent reduction in random error components. The effect of the adjustment is especially evident in RS, where the originally broad fluctuation range was compressed and brought into closer alignment with the dynamics of PS and CRNS (Figure 11).

The percentage of values falling within their respective WP–FC ranges changed only slightly for PS and CRNS (+1% each), whereas RS showed a decrease of 5%. This negative shift in RS performance can be attributed to the scaling procedure, which, in certain cases, displaced values downward, thereby pushing part of the distribution below the WP threshold.

A site-by-site analysis further highlights the flexibility of this method. In three out of the eight study sites, PS emerged

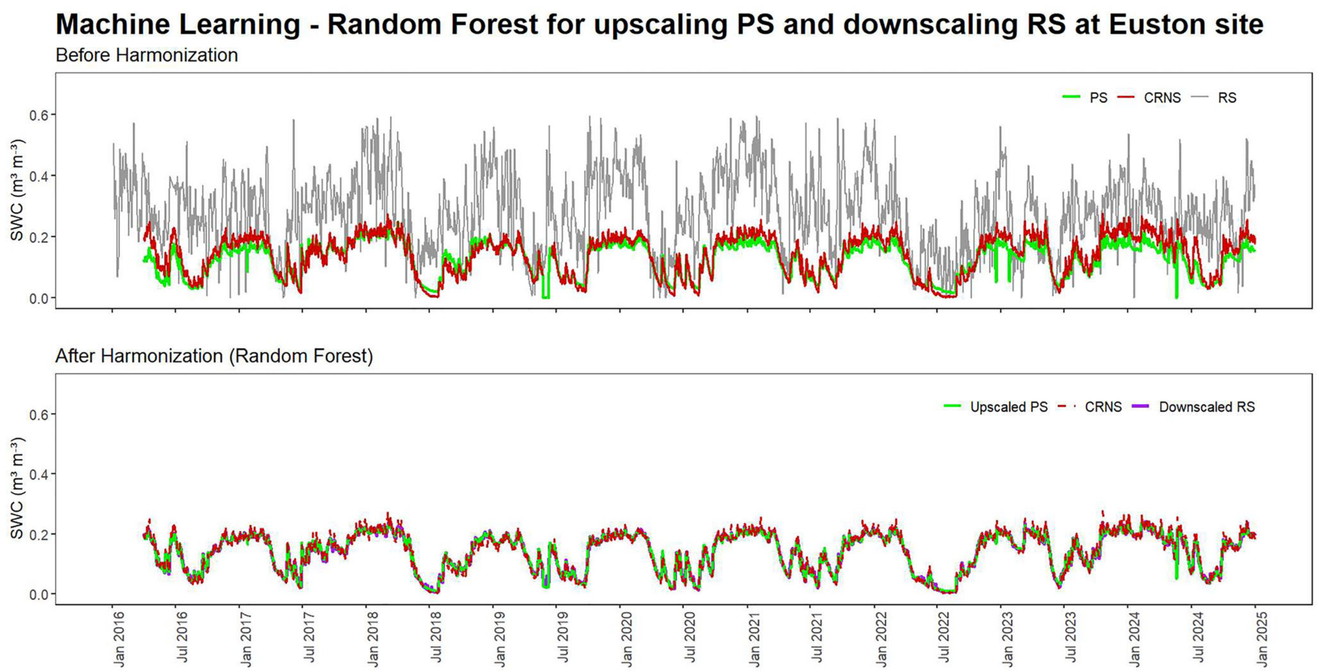

FIGURE 10 Time series of soil water content (SWC) from point-scale (PS), cosmic-ray neutron sensing (CRNS), and remote sensing (RS) before (top) and after (bottom) harmonization using random forest-based upscaling (PS) and downscaling (RS) to the CRNS footprint for the Euston site as an example.

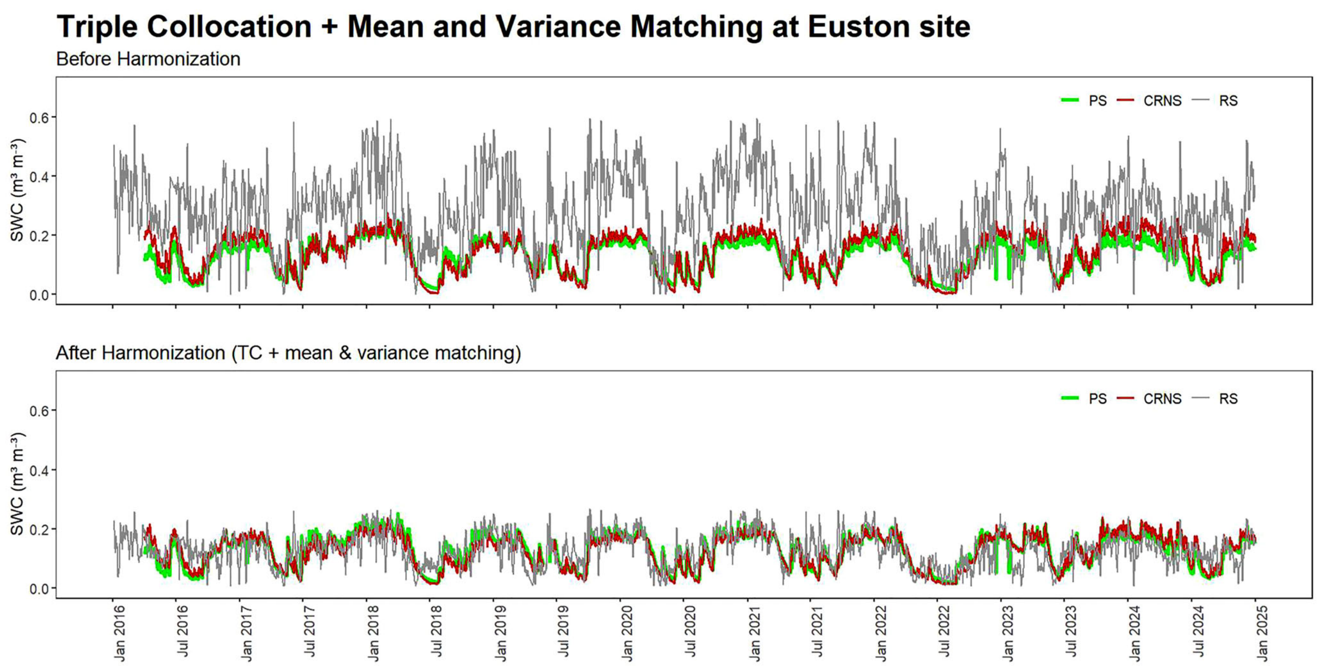

FIGURE 11 Soil water content (SWC) time series at the Euston site before (top) and after (bottom) applying the triple collocation (TC) method combined with mean and variance matching. CRNS, cosmic-ray neutron sensing; PS, point-scale; RS, remote sensing.

as the sensor with the lowest error variance and thus served as the scaling reference, whereas in the remaining five sites, CRNS provided the benchmark. This variability underlines the adaptive nature of the approach: the optimal reference sensor depends on local site conditions and sensor performance, ensuring that the harmonization process leverages the most reliable dataset available in each case.

The choice of lateral spatial harmonization method depends largely on the available data, particularly the number of PS measurements. Considering the methods feasible even with one PS sensor, the areal mean is the simplest approach. While it is easy to apply, it often leads to reduced accuracy because it ignores the spatial structure of the data, as shown by negative plausibility result changes in many cases. A more statistically robust option is TC with mean-variance matching. TC provides a strong statistical foundation by breaking down errors across datasets. It maintains dataset independence and can be used with a single PS sensor. However, a fundamental limitation of TC-based approaches is the requirement for three mutually independent data sources, which are not always available in practice; additionally, the associated scaling procedures can sometimes produce physically implausible values.

When multiple PS sensors are available, more sophisticated methods become viable. RF uses nonlinear relationships to improve alignment and can lead to significant increases in accuracy. However, RF's tendency to overfit and closely mimic PS trends can blur the line between harmonization and data combination, risking a loss of transparency. For more reliable and physically interpretable results, ordinary kriging is the superior choice. This method explicitly models spatial variability and provides marked improvements when sufficient PS data are available. The resulting synthetic CRNS and RS series closely mirror PS dynamics, which reduces the distinctiveness of each sensor type. While kriging yields the highest numerical results, its reliance on a dense network of sensors limits its broader applicability. Ultimately, the best method depends on balancing the trade-offs (Table 5) between data availability, desired interpretability, and the need for statistical alignment versus physical consistency.

4 | CONCLUSIONS

This study developed and evaluated a structured, four-step workflow for harmonizing SWC datasets from PS sensors, CRNS, and RS across seven European sites. For unit harmonization, total water storage capacity conversion outperformed mean-variance matching, yielding a higher proportion of RS values within physically plausible WP–FC ranges (37% vs. 35% with CRNS reference) while better preserving the natural variability of the RS signal. For temporal harmonization, daily averaging and satellite overpass selection produced nearly identical results (≈0% change for CRNS, ≈16% for PS), confirming that SWC memory renders subdaily temporal alignment choices largely inconsequential. Daily averaging was adopted for its fuller representation of diurnal variability. For depth harmonization, applying weighted averaging to PS and an exponential filter to RS improved RS plausibility by ≈12% and statistical agreement with CRNS ($\Delta R = +0.15$, ΔubRMSD $= -0.03$), with an average characteristic time length of ≈6 days across sites. For lateral spatial harmonization, method performance was strongly data-dependent. The areal mean is simple and requires only one PS sensor but disregards spatial structure, yielding a −6% plausibility change for CRNS on average. TC combined with mean-variance matching offers an error-aware alternative with minimal data requirements, though scaling can occasionally produce physically implausible values. RF captured nonlinear relationships effectively but showed signs of overfitting and blurred the boundary between harmonization and data fusion. Ordinary kriging produced the largest improvements where applicable (plausibility +16% for CRNS, +30% for RS; $\Delta R = +0.43$–0.44) but requires a sufficiently dense PS network and longer records; its results should otherwise be treated as exploratory.

Overall, no single method is universally optimal. The appropriate choice depends on data availability, the required balance between statistical alignment and physical consistency, and the risk of overfitting. The proposed framework provides a reproducible foundation for multi-sensor SWC intercomparison studies in hydrological and environmental applications.

AUTHOR CONTRIBUTIONS

Sadra Emamalizadeh: Conceptualization; data curation; formal analysis; methodology; visualization; writing—original draft; writing—review and editing. **Tim Howson**: Conceptualization; data curation; formal analysis; methodology; validation; writing—review and editing. **Riccardo Mazzoleni**: Data curation; validation; visualization; writing—review and editing. **Philip Vincent**: Methodology; supervision; writing—review and editing. **Jonathan G. Evans**: Methodology; supervision; writing—review and editing. **Gabriele Baroni**: Conceptualization; data curation; formal analysis; funding acquisition; methodology; supervision; writing—original draft; writing—review and editing.

ACKNOWLEDGMENTS

This research has been supported by the European Partnership on Metrology (funder ID, 10.13039/100019599; grant no. 21GRD08 SoMMet), co-financed from the European Union's Horizon Europe Research and Innovation Program and by the Participating States.

Open access publishing facilitated by Universita di Bologna, as part of the Wiley - CRUI-CARE agreement.

CONFLICT OF INTEREST STATEMENT

The authors declare no conflicts of interest.

DATA AVAILABILITY STATEMENT

Data have been uploaded to the following repository: https://doi.org/10.5281/zenodo.18038653.

ORCID

Sadra Emamalizadeh https://orcid.org/0009-0001-9307-3561

Riccardo Mazzoleni https://orcid.org/0000-0001-6461-5053
Philip Vincent https://orcid.org/0009-0006-0028-0956

REFERENCES

Abbaszadeh, P., Moradkhani, H., & Zhan, X. (2019). Downscaling SMAP radiometer soil moisture over the CONUS using an ensemble learning method. *Water Resources Research*, *55*(1), 324–344. https://doi.org/10.1029/2018WR023354

Abelen, S., & Seitz, F. (2013). Relating satellite gravimetry data to global soil moisture products via data harmonization and correlation analysis. *Remote Sensing of Environment*, *136*, 89–98. https://doi.org/10.1016/J.RSE.2013.04.012

Albergel, C., de Rosnay, P., Gruhier, C., Muñoz-Sabater, J., Hasenauer, S., Isaksen, L., Kerr, Y., & Wagner, W. (2012). Evaluation of remotely sensed and modelled soil moisture products using global ground-based in situ observations. *Remote Sensing of Environment*, *118*, 215–226. https://doi.org/10.1016/J.RSE.2011.11.017

Albergel, C., Rüdiger, C., Pellarin, T., Calvet, J. C., Fritz, N., Froissard, F., Suquia, D., Petitpa, A., Piguet, B., & Martin, E. (2008). From near-surface to root-zone soil moisture using an exponential filter: An assessment of the method based on in-situ observations and model simulations. *Hydrology and Earth System Sciences*, *12*(6), 1323–1337. https://doi.org/10.5194/HESS-12-1323-2008

Babaeian, E., Sadeghi, M., Jones, S. B., Montzka, C., Vereecken, H., & Tuller, M. (2019). Ground, proximal, and satellite remote sensing of soil moisture. *Reviews of Geophysics*, *57*(2), 530–616.

Baldwin, D., Manfreda, S., Lin, H., & Smithwick, E. A. H. (2019). Estimating root zone soil moisture across the Eastern United States with passive microwave satellite data and a simple hydrologic model. *Remote Sensing*, *11*(17), 2013. https://doi.org/10.3390/RS11172013

Baroni, G., & Oswald, S. E. (2015). A scaling approach for the assessment of biomass changes and rainfall interception using cosmic-ray neutron sensing. *Journal of Hydrology*, *525*, 264–276. https://doi.org/10.1016/J.JHYDROL.2015.03.053

Baroni, G., Scheiffele, L. M., Schrön, M., Ingwersen, J., & Oswald, S. E. (2018). Uncertainty, sensitivity and improvements in soil moisture estimation with cosmic-ray neutron sensing. *Journal of Hydrology*, *564*, 873–887. https://doi.org/10.1016/J.JHYDROL.2018.07.053

Bauer-Marschallinger, B., Freeman, V., Cao, S., Paulik, C., Schaufler, S., Stachl, T., Modanesi, S., Massari, C., Ciabatta, L., Brocca, L., & Wagner, W. (2019). Toward global soil moisture monitoring with Sentinel-1: Harnessing assets and overcoming obstacles. *IEEE Transactions on Geoscience and Remote Sensing*, *57*(1), 520–539. https://doi.org/10.1109/TGRS.2018.2858004

Bauer-Marschallinger, B., Paulik, C., Hochstöger, S., Mistelbauer, T., Modanesi, S., Ciabatta, L., Massari, C., Brocca, L., & Wagner, W. (2018). Soil moisture from fusion of scatterometer and SAR: Closing the scale gap with temporal filtering. *Remote Sensing*, *10*(7), 1030. https://doi.org/10.3390/rs10071030

Belgiu, M., & Drăguţ, L. (2016). Random forest in remote sensing: A review of applications and future directions. *ISPRS Journal of Photogrammetry and Remote Sensing*, *114*, 24–31. https://doi.org/10.1016/J.ISPRSJPRS.2016.01.011

Bogena, H. R., Huisman, J. A., Güntner, A., Hübner, C., Kusche, J., Jonard, F., Vey, S., & Vereecken, H. (2015). Emerging methods for noninvasive sensing of soil moisture dynamics from field to catchment scale: A review. *WIREs Water*, *2*(6), 635–647. https://doi.org/10.1002/WAT2.1097

Breiman, L. (2001). Random forests. *Machine Learning*, *45*(1), 5–32. https://doi.org/10.1023/A:1010933404324

Brocca, L., Ciabatta, L., Massari, C., Camici, S., & Tarpanelli, A. (2017). Soil moisture for hydrological applications: Open questions and new opportunities. *Water*, *9*(2), 140. https://doi.org/10.3390/W9020140

Brocca, L., Melone, F., Moramarco, T., & Morbidelli, R. (2010). Spatial-temporal variability of soil moisture and its estimation across scales. *Water Resources Research*, *46*(2), W02516. https://doi.org/10.1029/2009WR008016

Brown, W. G., Cosh, M. H., Dong, J., & Ochsner, T. E. (2023). Upscaling soil moisture from point scale to field scale: Toward a general model. *Vadose Zone Journal*, *22*(2), e20244. https://doi.org/10.1002/VZJ2.20244

Castanedo, F. (2013). A review of data fusion techniques. *The Scientific World Journal*, *2013*(1), 704504. https://doi.org/10.1155/2013/704504

Chen, F., Crow, W. T., Bindlish, R., Colliander, A., Burgin, M. S., Asanuma, J., & Aida, K. (2018). Global-scale evaluation of SMAP, SMOS and ASCAT soil moisture products using triple collocation. *Remote Sensing of Environment*, *214*, 1–13. https://doi.org/10.1016/J.RSE.2018.05.008

Choi, M., & Jacobs, J. M. (2011). Spatial soil moisture scaling structure during soil moisture experiment 2005. *Hydrological Processes*, *25*(6), 926–932. https://doi.org/10.1002/HYP.7877

Chrisman, B., & Zreda, M. (2013). Quantifying mesoscale soil moisture with the cosmic-ray rover. *Hydrology and Earth System Sciences*, *17*(12), 5097–5108. https://doi.org/10.5194/HESS-17-5097-2013

Colliander, A., Cosh, M. H., Misra, S., Jackson, T. J., Crow, W. T., Chan, S., Bindlish, R., Chae, C., Holifield Collins, C., & Yueh, S. H. (2017). Validation and scaling of soil moisture in a semi-arid environment: SMAP validation experiment 2015 (SMAPVEX15). *Remote Sensing of Environment*, *196*, 101–112. https://doi.org/10.1016/J.RSE.2017.04.022

Cooper, H. M., Bennett, E., Blake, J., Blyth, E., Boorman, D., Cooper, E., Evans, J., Fry, M., Jenkins, A., Morrison, R., Rylett, D., Stanley, S., Szczykulska, M., Trill, E., Antoniou, V., Askquith-Ellis, A., Ball, L., Brooks, M., Clarke, M. A., … Winterbourn, B. (2021). COSMOS-UK: National soil moisture and hydrometeorology data for environmental science research. *Earth System Science Data*, *13*(4), 1737–1757. https://doi.org/10.5194/ESSD-13-1737-2021

Crow, W. T., Berg, A. A., Cosh, M. H., Loew, A., Mohanty, B. P., Panciera, R., de Rosnay, P., Ryu, D., & Walker, J. P. (2012). Upscaling sparse ground-based soil moisture observations for the validation of coarse-resolution satellite soil moisture products. *Reviews of Geophysics*, *50*(2), RG2002. https://doi.org/10.1029/2011RG000372

Delval, L., Vanderborght, J., & Javaux, M. (2025). Combination of plant and soil water potential monitoring and modelling demonstrates soil-root hydraulic disconnection during drought. *Plant and Soil*, *511*(1), 1449–1472. https://doi.org/10.1007/s11104-024-07062-2

Dorigo, W., de Jeu, R., Chung, D., Parinussa, R., Liu, Y., Wagner, W., & Fernández-Prieto, D. (2012). Evaluating global trends (1988–2010) in harmonized multi-satellite surface soil moisture. *Geophysical Research Letters*, *39*(18), L18405. https://doi.org/10.1029/2012GL052988

Dorigo, W. A., Xaver, A., Vreugdenhil, M., Gruber, A., Hegyiová, A., Sanchis-Dufau, A. D., Zamojski, D., Cordes, C., Wagner, W., & Drusch, M. (2013). Global automated quality control of in situ soil moisture data from the international soil moisture network. *Vadose Zone Journal*, *12*(3), 1–21. https://doi.org/10.2136/vzj2012.0097

Duygu, M. B., & Akyürek, Z. (2019). Using cosmic-ray neutron probes in validating satellite soil moisture products and land surface models. *Water*, *11*(7), 1362. https://doi.org/10.3390/W11071362

Emamalizadeh, S., Pirola, A., Alessandrini, C., Balenzano, A., & Baroni, G. (2024). Comparison of soil water content from SCATSAR-SWI and cosmic ray neutron sensing at four agricultural sites in Northern Italy: Insights from spatial variability and representativeness. *Remote Sensing*, *16*(18), 3384. https://doi.org/10.3390/RS16183384

Entekhabi, D., Njoku, E. G., O'Neill, P. E., Kellogg, K. H., Crow, W. T., Edelstein, W. N., Entin, J. K., Goodman, S. D., Jackson, T. J., Johnson, J., Kimball, J., Piepmeier, J. R., Koster, R. D., Martin, N., McDonald, K. C., Moghaddam, M., Moran, S., Reichle, R., Shi, J. C., … Van Zyl, J. (2010). The soil moisture active passive (SMAP) mission. *Proceedings of the IEEE*, *98*(5), 704–716. https://doi.org/10.1109/JPROC.2010.2043918

Entekhabi, D., Rodriguez-Iturbe, I., & Castelli, F. (1996). Mutual interaction of soil moisture state and atmospheric processes. *Journal of Hydrology*, *184*(1–2), 3–17. https://doi.org/10.1016/0022-1694(95)02965-6

Fang, B., Lakshmi, V., Bindlish, R., & Jackson, T. J. (2018). Downscaling of SMAP soil moisture using land surface temperature and vegetation data. *Vadose Zone Journal*, *17*(1), 1–15. https://doi.org/10.2136/VZJ2017.11.0198

Ford, T. W., Harris, E., & Quiring, S. M. (2014). Estimating root zone soil moisture using near-surface observations from SMOS. *Hydrology and Earth System Sciences*, *18*(1), 139–154. https://doi.org/10.5194/HESS-18-139-2014

Franz, T. E., Zreda, M., Ferre, T. P. A., Rosolem, R., Zweck, C., Stillman, S., Zeng, X., & Shuttleworth, W. J. (2012). Measurement depth of the cosmic ray soil moisture probe affected by hydrogen from various sources. *Water Resources Research*, *48*(8), W08515. https://doi.org/10.1029/2012WR011871

Ge, X., Ding, J., Jin, X., Wang, J., Chen, X., Li, X., Liu, J., & Xie, B. (2021). Estimating agricultural soil moisture content through UAV-based hyperspectral images in the arid region. *Remote Sensing*, *13*(8), 1562. https://doi.org/10.3390/RS13081562/S1

Gibon, F., Mialon, A., Richaume, P., Rodríguez-Fernández, N., Aberer, D., Boresch, A., Crapolicchio, R., Dorigo, W., Gruber, A., Himmelbauer, I., Preimesberger, W., Sabia, R., Stradiotti, P., Tercjak, M., & Kerr, Y. H. (2024). Estimating the uncertainties of satellite derived soil moisture at global scale. *Science of Remote Sensing*, *10*, 100147. https://doi.org/10.1016/J.SRS.2024.100147

Gruber, A., Dorigo, W. A., Zwieback, S., Xaver, A., & Wagner, W. (2013). characterizing coarse-scale representativeness of in situ soil moisture measurements from the international soil moisture network. *Vadose Zone Journal*, *12*(2), 1–16. https://doi.org/10.2136/VZJ2012.0170

Heathman, G. C., Cosh, M. H., Han, E., Jackson, T. J., McKee, L., & McAfee, S. (2012). Field scale spatiotemporal analysis of surface soil moisture for evaluating point-scale in situ networks. *Geoderma*, *170*, 195–205. https://doi.org/10.1016/J.GEODERMA.2011.11.004

Heathman, G. C., Cosh, M. H., Merwade, V., & Han, E. (2012). Multi-scale temporal stability analysis of surface and subsurface soil moisture within the Upper Cedar Creek Watershed, Indiana. *Catena*, *95*, 91–103. https://doi.org/10.1016/J.CATENA.2012.03.008

Heistermann, M., Francke, T., Scheiffele, L., Petrova, K. D., Budach, C., Schrön, M., Trost, B., Rasche, D., Güntner, A., Döpper, V., Förster, M., Köhli, M., Angermann, L., Antonoglou, N., Zude-Sasse, M., & Oswald, S. (2023). Three years of soil moisture observations by a dense cosmic-ray neutron sensing cluster at an agricultural research site in north-east Germany. *Earth System Science Data*, *15*, 3243–3262. https://doi.org/10.5194/ESSD-2023-19

Iwema, J., Rosolem, R., Rahman, M., Blyth, E., & Wagener, T. (2017). Land surface model performance using cosmic-ray and point-scale soil moisture measurements for calibration. *Hydrology and Earth System Sciences*, *21*(6), 2843–2861. https://doi.org/10.5194/HESS-21-2843-2017

Jacobs, J. (2004). SMEX02: Field scale variability, time stability and similarity of soil moisture. *Remote Sensing of Environment*, *92*(4), 436–446. https://doi.org/10.1016/J.RSE.2004.02.017

Kang, J., Jin, R., Li, X., Zhang, Y., & Zhu, Z. (2018). Spatial upscaling of sparse soil moisture observations based on ridge regression. *Remote Sensing*, *10*(2), 192. https://doi.org/10.3390/RS10020192

Kędzior, M., & Zawadzki, J. (2016). Comparative study of soil moisture estimations from SMOS satellite mission, GLDAS database, and cosmic-ray neutrons measurements at COSMOS station in Eastern Poland. *Geoderma*, *283*, 21–31. https://doi.org/10.1016/J.GEODERMA.2016.07.023

Kerr, Y. H., Waldteufel, P., Wigneron, J.-P., Delwart, S., Cabot, F., Boutin, J., Escorihuela, M.-J., Font, J., Reul, N., Gruhier, C., Juglea, S. E., Drinkwater, M. R., Hahne, A., Martín-Neira, M., & Mecklenburg, S. (2010). The SMOS L: New tool for monitoring key elements of the global water cycle. *Proceedings of the IEEE*, *98*(5), 666–687. https://doi.org/10.1109/JPROC.2010.2043032

Köhli, M., Schrön, M., Zreda, M., Schmidt, U., Dietrich, P., & Zacharias, S. (2015). Footprint characteristics revised for field-scale soil moisture monitoring with cosmic-ray neutrons. *Water Resources Research*, *51*(7), 5772–5790. https://doi.org/10.1002/2015WR017169

Krueger, E. S., & Ochsner, T. E. (2024). Traditional matric potential thresholds underestimate soil moisture at field capacity across Oklahoma. *Soil Science Society of America Journal*, *88*(5), 1678–1690. https://doi.org/10.1002/saj2.20733

Kuhlmann, A., Neuweiler, I., Van Der Zee, S. E. A. T. M., & Helmig, R. (2012). Influence of soil structure and root water uptake strategy on unsaturated flow in heterogeneous media. *Water Resources Research*, *48*(2), 2534. https://doi.org/10.1029/2011WR010651

Leroux, C., Jones, H., Pichon, L., Taylor, J., & Tisseyre, B. (2019). Automatic harmonization of heterogeneous agronomic and environmental spatial data. *Precision Agriculture*, *20*(6), 1211–1230. https://doi.org/10.1007/S11119-019-09650-0/METRICS

Li, J., & Zhang, L. (2021). Comparison of four methods for vertical extrapolation of soil moisture contents from surface to deep layers in an alpine area. *Sustainability*, *13*(16), 8862. https://doi.org/10.3390/SU13168862

Li, T., Jeřábek, J., Noreika, N., Dostál, T., & Zumr, D. (2021). An overview of hydrometeorological datasets from a small agricultural catchment (Nučice) in the Czech Republic. *Hydrological Processes*, *35*(2), e14042. https://doi.org/10.1002/hyp.14042

Liu, D., Wang, G., Mei, R., Yu, Z., & Yu, M. (2014). Impact of initial soil moisture anomalies on climate mean and extremes over Asia. *Journal of Geophysical Research: Atmospheres*, *119*(2), 529–545. https://doi.org/10.1002/2013JD020890

Liu, J., Rahmani, F., Lawson, K., & Shen, C. (2022). A multiscale deep learning model for soil moisture integrating satellite and in situ data. *Geophysical Research Letters*, *49*(7), e2021GL096847. https://doi.org/10.1029/2021GL096847

Liu, L., Gudmundsson, L., Hauser, M., Qin, D., Li, S., & Seneviratne, S. I. (2020). Soil moisture dominates dryness stress on ecosystem production globally. *Nature Communications*, *11*(1), Article 4892. https://doi.org/10.1038/S41467-020-18631-1

Liu, Y., Yang, Y., Jing, W., & Yue, X. (2017). Comparison of different machine learning approaches for monthly satellite-based soil moisture downscaling over Northeast China. *Remote Sensing*, *10*(1), 31. https://doi.org/10.3390/RS10010031

Madelon, R., Rodríguez-Fernández, N. J., Bazzi, H., Baghdadi, N., Albergel, C., Dorigo, W., & Zribi, M. (2023). Soil moisture estimates at 1 km resolution making a synergistic use of sentinel data. *Hydrology and Earth System Sciences*, *27*(6), 1221–1242. https://doi.org/10.5194/HESS-27-1221-2023

Mälicke, M., Hassler, S. K., Blume, T., Weiler, M., & Zehe, E. (2020). Soil moisture: Variable in space but redundant in time. *Hydrology and Earth System Sciences*, *24*(5), 2633–2653. https://doi.org/10.5194/hess-24-2633-2020

Markonis, Y., Pappas, C., Hanel, M., & Papalexiou, S. M. (2021). A cross-scale framework for integrating multi-source data in earth system sciences. *Environmental Modelling & Software*, *139*, 104997. https://doi.org/10.1016/J.ENVSOFT.2021.104997

Massari, C., Brocca, L., Tarpanelli, A., & Moramarco, T. (2015). Data assimilation of satellite soil moisture into rainfall-runoff modelling: A complex recipe? *Remote Sensing*, *7*(9), 11403–11433. https://doi.org/10.3390/RS70911403

Mazzoleni, R., Emamalizadeh, S., & Baroni, G. (2025). *Datasets analyzed within the study "cosmic-ray neutron sensing to monitor soil moisture across various irrigation methods*." Zenodo. https://doi.org/10.5281/ZENODO.17177047

McJannet, D., Hawdon, A., Baker, B., Renzullo, L., & Searle, R. (2017). Multiscale soil moisture estimates using static and roving cosmic-ray soil moisture sensors. *Hydrology and Earth System Sciences*, *21*(12), 6049–6067. https://doi.org/10.5194/HESS-21-6049-2017

Minasny, B., & McBratney, A. B. (2016). Digital soil mapping: A brief history and some lessons. *Geoderma*, *264*, 301–311. https://doi.org/10.1016/J.GEODERMA.2015.07.017

Montzka, C., Bogena, H. R., Zreda, M., Monerris, A., Morrison, R., Muddu, S., & Vereecken, H. (2017). Validation of spaceborne and modelled surface soil moisture products with cosmic-ray neutron probes. *Remote Sensing*, *9*(2), 103. https://doi.org/10.3390/RS9020103

Nguyen, H. H., Jeong, J., & Choi, M. (2019). Extension of cosmic-ray neutron probe measurement depth for improving field scale root-zone soil moisture estimation by coupling with representative in-situ sensors. *Journal of Hydrology*, *571*, 679–696. https://doi.org/10.1016/J.JHYDROL.2019.02.018

Ochsner, T. E., Cosh, M. H., Cuenca, R. H., Dorigo, W. A., Draper, C. S., Hagimoto, Y., Kerr, Y. H., Larson, K. M., Njoku, E. G., Small, E. E., & Zreda, M. (2013). State of the art in large-scale soil moisture monitoring. *Soil Science Society of America Journal*, *77*(6), 1888–1919. https://doi.org/10.2136/SSSAJ2013.03.0093

Pauwels, V. R. N., Hoeben, R., Verhoest, N. E. C., & De Troch, F. P. (2001). The importance of the spatial patterns of remotely sensed soil moisture in the improvement of discharge predictions for small-scale basins through data assimilation. *Journal of Hydrology*, *251*(1–2), 88–102. https://doi.org/10.1016/S0022-1694(01)00440-1

Peng, J., Albergel, C., Balenzano, A., Brocca, L., Cartus, O., Cosh, M. H., Crow, W. T., Dabrowska-Zielinska, K., Dadson, S., Davidson, M. W. J., de Rosnay, P., Dorigo, W., Gruber, A., Hagemann, S., Hirschi, M., Kerr, Y. H., Lovergine, F., Mahecha, M. D., Marzahn, P., … Loew, A. (2021). A roadmap for high-resolution satellite soil moisture applications—Confronting product characteristics with user requirements. *Remote Sensing of Environment*, *252*, 112162. https://doi.org/10.1016/J.RSE.2020.112162

Peng, J., Tanguy, M., Robinson, E. L., Pinnington, E., Evans, J., Ellis, R., Cooper, E., Hannaford, J., Blyth, E., & Dadson, S. (2021). Estimation and evaluation of high-resolution soil moisture from merged model and earth observation data in the Great Britain. *Remote Sensing of Environment*, *264*, 112610. https://doi.org/10.1016/J.RSE.2021.112610

Poggio, L., de Sousa, L. M., Batjes, N. H., Heuvelink, G. B. M., Kempen, B., Ribeiro, E., & Rossiter, D. (2021). SoilGrids 2.0: Producing soil information for the globe with quantified spatial uncertainty. *soil*, *7*(1), 217–240. https://doi.org/10.5194/SOIL-7-217-2021

Power, D., Rico-Ramirez, M. A., Desilets, S., Desilets, D., & Rosolem, R. (2021). Cosmic-ray neutron sensor PYthon tool (Crspy 1.2.1): An open-source tool for the processing of cosmic-ray neutron and soil moisture data. *Geoscientific Model Development*, *14*(12), 7287–7307. https://doi.org/10.5194/GMD-14-7287-2021

Qiu, J., He, C., Liu, X., Gao, L., Tan, C., Wang, X., Kong, D., Wigneron, J. P., Chen, D., & Xia, J. (2024). Projecting dry-wet abrupt alternation across China from the perspective of soil moisture. *Npj Climate and Atmospheric Science*, *7*(1), Article 269. https://doi.org/10.1038/S41612-024-00808-W;SUBJMETA

Rahmati, M., Amelung, W., Brogi, C., Dari, J., Flammini, A., Bogena, H., Brocca, L., Chen, H., Groh, J., Koster, R. D., McColl, K. A., Montzka, C., Moradi, S., Rahi, A., Sharghi, S. F., & Vereecken, H. (2024). Soil moisture memory: State-of-the-art and the way forward. *Reviews of Geophysics*, *62*(2), e2023RG000828. https://doi.org/10.1029/2023RG000828

Reichle, R. H., & Koster, R. D. (2004). Bias reduction in short records of satellite soil moisture. *Geophysical Research Letters*, *31*(19), L19501. https://doi.org/10.1029/2004GL020938

Richards, L. A. (1931). Capillary conduction of liquids through porous mediums. *Journal of Applied Physics*, *1*(5), 318–33. https://doi.org/10.1063/1.1745010

Rivera Villarreyes, C. A., Baroni, G., & Oswald, S. E. (2014). Inverse modelling of cosmic-ray soil moisture for field-scale soil hydraulic parameters. *European Journal of Soil Science*, *65*(6), 876–886. https://doi.org/10.1111/EJSS.12162

Robinson, D. A., Campbell, C. S., Hopmans, J. W., Hornbuckle, B. K., Jones, S. B., Knight, R., Ogden, F., Selker, J., & Wendroth, O. (2008). Soil moisture measurement for ecological and hydrological watershed-scale observatories: A review. *Vadose Zone Journal*, *7*(1), 358–389. https://doi.org/10.2136/VZJ2007.0143

Rud, J. A. P., Ochsner, T. E., & Patrignani, A. (2024). CRNPy: An open-source python library for cosmic-ray neutron probe data processing. *Journal of Open Source Software*, *9*(97), 6025. https://doi.org/10.21105/JOSS.06025

Saxton, K. E., & Rawls, W. J. (2006). Soil water characteristic estimates by texture and organic matter for hydrologic solutions. *Soil Science Society of America Journal*, *70*(5), 1569–1578. https://doi.org/10.2136/SSSAJ2005.0117;CTYPE:STRING:JOURNAL

Scheiffele, L. M., Munz, M., Francke, T., Baroni, G., & Oswald, S. E. (2025). Enhancing hectare-scale groundwater recharge estimation by integrating data from cosmic-ray neutron sensing into soil hydrological modeling. *Water Resources Research*, *61*(1), e2024WR037641. https://doi.org/10.1029/2024WR037641

Schmidt, T., Schrön, M., Li, Z., Francke, T., Zacharias, S., Hildebrandt, A., & Peng, J. (2024). Comprehensive quality assessment of satellite-and model-based soil moisture products against the COSMOS network in Germany. *Remote Sensing of Environment*, *301*, 113930. https://doi.org/10.1016/J.RSE.2023.113930

Schrön, M., Köhli, M., Scheiffele, L., Iwema, J., Bogena, H. R., Lv, L., Martini, E., Baroni, G., Rosolem, R., Weimar, J., Mai, J., Cuntz, M., Rebmann, C., Oswald, S. E., Dietrich, P., Schmidt, U., & Zacharias, S. (2017). Improving calibration and validation of cosmic-ray neutron sensors in the light of spatial sensitivity. *Hydrology and Earth System Sciences*, *21*(10), 5009–5030. https://doi.org/10.5194/hess-21-5009-2017

Senanayake, I. P., Yeo, I. Y., Walker, J. P., & Willgoose, G. R. (2021). Estimating catchment scale soil moisture at a high spatial resolution: Integrating remote sensing and machine learning. *Science of the Total Environment*, *776*, 145924. https://doi.org/10.1016/J.SCITOTENV.2021.145924

Seneviratne, S. I., Corti, T., Davin, E. L., Hirschi, M., Jaeger, E. B., Lehner, I., Orlowsky, B., & Teuling, A. J. (2010). Investigating soil moisture–climate interactions in a changing climate: A review. *Earth-Science Reviews*, *99*(3–4), 125–161. https://doi.org/10.1016/J.EARSCIREV.2010.02.004

Senyurek, V., Farhad, M. M., Gurbuz, A. C., Kurum, M., & Adeli, A. (2022). Fusion of reflected GPS signals with multispectral imagery to estimate soil moisture at subfield scale from small UAS platforms. *IEEE Journal of Selected Topics in Applied Earth Observations and Remote Sensing*, *15*, 6843–6855. https://doi.org/10.1109/JSTARS.2022.3197794

Seo, M.-G., Shin, H.-S., & Tsourdos, A. (2021). Soil Moisture retrieval model design with multispectral and infrared images from unmanned aerial vehicles using convolutional neural network. *Agronomy*, *11*(2), 398. https://doi.org/10.3390/AGRONOMY11020398

Shinoda, M., & Nandintsetseg, B. (2011). Soil moisture and vegetation memories in a cold, arid climate. *Global and Planetary Change*, *79*(1–2), 110–117. https://doi.org/10.1016/J.GLOPLACHA.2011.08.005

Stoffelen, A. (1998). Toward the true near-surface wind speed: Error modeling and calibration using triple collocation. *Journal of Geophysical Research: Oceans*, *103*(3334), 7755–7766. https://doi.org/10.1029/97JC03180

Szabó, B., Weynants, M., & Weber, T. K. D. (2021). Updated European hydraulic pedotransfer functions with communicated uncertainties in the predicted variables (euptfv2). *Geoscientific Model Development*, *14*(1), 151–175. https://doi.org/10.5194/GMD-14-151-2021

Tunçay, T. (2021). Comparison quality of interpolation methods to estimate spatial distribution of soil moisture content. *Communications in Soil Science and Plant Analysis*, *52*(4), 353–374. https://doi.org/10.1080/00103624.2020.1854283

Ulaby, F. T., Dubois, P. C., & Van Zyl, J. (1996). Radar mapping of surface soil moisture. *Journal of Hydrology*, *184*, 57–84.

Upadhyaya, D. B., Evans, J., Muddu, S., Tomer, S. K., Al Bitar, A., Yeggina, S., S, T., Morrison, R., Fry, M., Tripathi, S. N., Mujumdar, M., Goswami, M., Ganeshi, N., Nema, M. K., Jain, S. K., Angadi, S. S., & Yenagi, B. S. (2021). The Indian COSMOS Network (ICON): Validating L-band remote sensing and modelled soil moisture data products. *Remote Sensing*, *13*(3), 537. https://doi.org/10.3390/RS13030537

Usowicz, B., Lukowski, M., & Lipiec, J. (2020). The SMOS-derived soil water extent and equivalent layer thickness facilitate determination of soil water resources. *Scientific Reports*, *10*(1), 1–12. https://doi.org/10.1038/s41598-020-75475-x

Vachaud, G., Passerat De Silans, A., Balabanis, P., & Vauclin, M. (1985). Temporal stability of spatially measured soil water probability density function. *Soil Science Society of America Journal*, *49*(4), 822–828. https://doi.org/10.2136/sssaj1985.03615995004900040006x

van Genuchten, M. T. (1980). A closed-form equation for predicting the hydraulic conductivity of unsaturated soils. *Soil Science Society of America Journal*, *44*(5), 892–898. https://doi.org/10.2136/SSSAJ1980.03615995004400050002X

Vereecken, H., Huisman, J. A., Bogena, H., Vanderborght, J., Vrugt, J. A., & Hopmans, J. W. (2008). On the value of soil moisture measurements in vadose zone hydrology: A review. *Water Resources Research*, *44*(4), W00D06. https://doi.org/10.1029/2008WR006829

Wackernagel, H. (2003). *Multivariate geostatistics: An introduction with applications*. Springer. https://doi.org/10.1007/978-3-662-05294-5

Wagner, W., Hahn, S., Kidd, R., Melzer, T., Bartalis, Z., Hasenauer, S., Figa-Saldaña, J., de Rosnay, P., Jann, A., Schneider, S., Komma, J., Kubu, G., Brugger, K., Aubrecht, C., Züger, J., Gangkofner, U., Kienberger, S., Brocca, L., Wang, Y., … Steinnocher, K. (2013). The ASCAT soil moisture product: A review of its specifications, validation results, and emerging applications. *Meteorologische Zeitschriftt*, *22*(1), 5–33.

Wagner, W., Lemoine, G., & Rott, H. (1999). A method for estimating soil moisture from ERS scatterometer and soil data. *Remote Sensing of Environment*, *70*(2), 191–207. https://doi.org/10.1016/S0034-4257(99)00036-X

Wang, Y., Mao, J., Jin, M., Hoffman, F. M., Shi, X., Wullschleger, S. D., & Dai, Y. (2021). Development of observation-based global multilayer soil moisture products for 1970 to 2016. *Earth System Science Data*, *13*(9), 4385–4405. https://doi.org/10.5194/ESSD-13-4385-2021

Webster, R., & Oliver, M. A. (2008). *Geostatistics for environmental scientists* (2nd ed.). John Wiley & Sons, Ltd. https://doi.org/10.1002/9780470517277

Western, A. W., & Blöschl, G. (1999). On the spatial scaling of soil moisture. *Journal of Hydrology*, *217*(3–4), 203–224. https://doi.org/10.1016/S0022-1694(98)00232-7

Wösten, J. H. M., Lilly, A., Nemes, A., & Bas, C. L. (1999). Development and use of a database of hydraulic properties of European soils. *Geoderma*, *90*(3–4), 169–185. https://doi.org/10.1016/S0016-7061(98)00132-3

Wu, D., Andales, A. A., Yang, H., Sun, Q., Chen, S., Guo, X., Li, D., & Du, T. (2021). Linking crop water productivity to soil physical, chemical and microbial properties. *Frontiers of Agricultural Science and Engineering*, *8*(4), 545–558. https://doi.org/10.15302/J-FASE-2020349

Wu, K., Ryu, D., Wagner, W., & Hu, Z. (2023). A global-scale intercomparison of triple collocation analysis- and ground-based soil moisture time-variant errors derived from different rescaling techniques. *Remote Sensing of Environment*, *285*, 113387. https://doi.org/10.1016/J.RSE.2022.113387

Xie, B., Jia, X., Qin, Z., Zhao, C., & Shao, M. (2020). Comparison of interpolation methods for soil moisture prediction on China's Loess Plateau. *Vadose Zone Journal*, *19*(1), e20025. https://doi.org/10.1002/vzj2.20025

Xie, J., Ding, L., Wang, X., Qin, W., Xu, H., & Zhang, M. (2025). Comparison of spatial interpolation methods for rainfall erosivity in a typical basin in the Hengduan Mountain region, Southwest China. *Ecological Indicators*, *174*, 113451. https://doi.org/10.1016/J.ECOLIND.2025.113451

Yan, R., & Bai, J. (2020). A new approach for soil moisture downscaling in the presence of seasonal difference. *Remote Sensing*, *12*(17), 2818. https://doi.org/10.3390/RS12172818

Yuan, Q., Xu, H., Li, T., Shen, H., & Zhang, L. (2020). Estimating surface soil moisture from satellite observations using a generalized regression neural network trained on sparse ground-based measurements in the continental U.S. *Journal of Hydrology*, *580*, 124351. https://doi.org/10.1016/J.JHYDROL.2019.124351

Zhang, D., Zhang, W., Huang, W., Hong, Z., & Meng, L. (2017). Upscaling of surface soil moisture using a deep learning model with VIIRS RDR. *ISPRS International Journal of Geo-Information*, *6*(5), 130. https://doi.org/10.3390/IJGI6050130

Zhang, N., Quiring, S., Ochsner, T., & Ford, T. (2017). Comparison of three methods for vertical extrapolation of soil moisture in Oklahoma. *Vadose Zone Journal*, *16*(10), 1–19. https://doi.org/10.2136/VZJ2017.04.0085

Zhang, Y., Han, W., Zhang, H., Niu, X., & Shao, G. (2023). Evaluating soil moisture content under maize coverage using UAV multimodal data by machine learning algorithms. *Journal of Hydrology*, *617*, 129086. https://doi.org/10.1016/J.JHYDROL.2023.129086

Zhao, H., Montzka, C., Vereecken, H., & Franssen, H. J. H. (2024). A comparative analysis of remote sensing soil moisture datasets fusion methods: Novel LSTM approach versus widely used triple collocation technique. *IEEE Journal of Selected Topics in Applied Earth Observations and Remote Sensing*, *17*, 16659–16671. https://doi.org/10.1109/JSTARS.2024.3455549

Zheng, Y., Coxon, G., Woods, R., Power, D., Rico-Ramirez, M. A., McJannet, D., Rosolem, R., Li, J., & Feng, P. (2024). Evaluation of reanalysis soil moisture products using cosmic ray neutron sensor observations across the globe. *Hydrology and Earth System Sciences*, *28*(9), 1999–2022. https://doi.org/10.5194/HESS-28-1999-2024

Zheng, Z., Zhang, F., Chai, X., Zhu, Z., & Ma, F. (2009). Spatial estimation of soil moisture and salinity with neural kriging. *IFIP International Federation for Information Processing*, *294*, 1227–1237. https://doi.org/10.1007/978-1-4419-0211-5_51

Zhu, L., Li, W., Wang, H., Deng, X., Tong, C., He, S., & Wang, K. (2023). Merging microwave, optical, and reanalysis data for 1 km daily soil moisture by triple collocation. *Remote Sensing*, *15*(1), 159. https://doi.org/10.3390/RS15010159/S1

Zhu, X., Chen, J., Gao, F., Chen, X., & Masek, J. G. (2010). An enhanced spatial and temporal adaptive reflectance fusion model for complex heterogeneous regions. *Remote Sensing of Environment*, *114*(11), 2610–2623. https://doi.org/10.1016/J.RSE.2010.05.032

Zreda, M., Desilets, D., Ferré, T. P. A., & Scott, R. L. (2008). Measuring soil moisture content non-invasively at intermediate spatial scale using cosmic-ray neutrons. *Geophysical Research Letters*, *35*(21), L21402. https://doi.org/10.1029/2008GL035655

Zreda, M., Shuttleworth, W. J., Zeng, X., Zweck, C., Desilets, D., Franz, T., & Rosolem, R. (2012). COSMOS: The cosmic-ray soil moisture observing system. *Hydrology and Earth System Sciences*, *16*(11), 4079–4099. https://doi.org/10.5194/HESS-16-4079-2012

How to cite this article: Emamalizadeh, S., Howson, T., Mazzoleni, R., Vincent, P., Evans, J. G., & Baroni, G. (2026). Toward a structured workflow to harmonize soil water content products: A comparative study across different methods. *Vadose Zone Journal*, *25*, e70127. https://doi.org/10.1002/vzj2.70127

APPENDIX

LITERATURE REVIEW OF SOIL WATER CONTENT (SWC) HARMONIZATION STUDIES, FOCUSING ON THE CONSIDERED COMPONENTS AND THEIR RESPECTIVE CATEGORIES. In the table, a marked cell indicates that the corresponding harmonization component is applied in the study, while an unmarked (blank) cell indicates that it is not applied

Number	Reference	Harmonization component/element				Harmonization category				
		Unit	Temporal	Depth	Lateral spatial	General statistical	Spatial statistical	Machine learning	Triple collocation	Process-based
1.	(Abbaszadeh et al., 2019)	☐	☒	☐	☒	☐	☐	☒	☐	☐
2.	(Abelen & Seitz, 2013)	☒	☒	☐	☒	☒	☐	☐	☐	☐
3.	(Albergel et al., 2008)	☒	☒	☒	☒	☒	☐	☐	☐	☐
4.	(Baldwin et al., 2019)	☒	☒	☒	☒	☒	☒	☒	☐	☒
5.	(Bauer-Marschallinger et al., 2019)	☒	☒	☐	☒	☒	☒	☒	☐	☐
6.	(Brocca et al., 2010)	☐	☒	☐	☒	☒	☒	☐	☐	☐
7.	(Brown et al., 2023)	☐	☒	☒	☒	☒	☒	☐	☐	☐
8.	(Chen et al., 2018)	☒	☒	☐	☐	☒	☐	☐	☒	☐
9.	(Choi & Jacobs, 2011)	☐	☐	☐	☒	☒	☐	☐	☐	☐
10.	(Chrisman & Zreda, 2013)	☐	☒	☐	☒	☐	☒	☐	☐	☐
11.	(Crow et al., 2012)	☒	☐	☐	☒	☒	☒	☐	☐	☐
12.	(D. Zhang, Zhang, et al., 2017)	☐	☒	☐	☒	☐	☐	☒	☐	☐
13.	(Duygu & Akyürek, 2019)	☒	☒	☐	☐	☐	☐	☐	☒	☐
14.	(Fang et al., 2018)	☐	☒	☐	☒	☒	☒	☐	☐	☐
15.	(Franz et al., 2012)	☐	☐	☒	☐	☒	☐	☐	☐	☒
16.	(Ge et al., 2021)	☐	☒	☐	☒	☐	☐	☒	☐	☐
17.	(Gibon et al., 2024)	☐	☐	☐	☒	☐	☒	☐	☒	☐
18.	(Gruber et al., 2013)	☐	☒	☐	☒	☒	☐	☐	☒	☐
19.	(Heathman, Cosh, Han, et al., 2012)	☐	☒	☐	☒	☒	☒	☐	☐	☐
20.	(Iwema et al., 2017)	☒	☐	☒	☒	☐	☐	☐	☐	☒
21.	(Jacobs et al., 2004)	☐	☒	☐	☒	☒	☒	☐	☐	☐
22.	(Kang et al., 2018)	☐	☐	☐	☒	☒	☐	☐	☐	☐
23.	(Kędzior & Zawadzki, 2016)	☐	☐	☒	☐	☒	☐	☐	☒	☐
24.	(Leroux et al., 2019)	☐	☒	☐	☒	☒	☒	☐	☐	☐
25.	(J. Li & Zhang, 2021)	☐	☐	☒	☐	☒	☐	☒	☐	☐
26.	(Y. Liu et al., 2017)	☐	☒	☐	☒	☐	☐	☒	☐	☐
27.	(J. Liu et al., 2022)	☒	☐	☐	☒	☐	☐	☒	☐	☐
28.	(Madelon et al., 2023)	☒	☒	☐	☒	☒	☐	☒	☐	☒
29.	(Markonis et al., 2021)	☐	☒	☐	☒	☒	☒	☐	☐	☐
30.	(Massari et al., 2015)	☒	☒	☒	☒	☒	☐	☐	☐	☒
31.	(McJannet et al., 2017)	☐	☐	☐	☒	☐	☒	☐	☐	☐
32.	(Montzka et al., 2017)	☒	☒	☐	☒	☒	☐	☐	☒	☐
33.	(N. Zhang, Quiring, et al., 2017)	☐	☒	☒	☒	☒	☐	☐	☐	☐

(Continues)

Number	Reference	Harmonization component/element				Harmonization category				
		Unit	Temporal	Depth	Lateral spatial	General statistical	Spatial statistical	Machine learning	Triple collocation	Process-based
34.	(Nguyen et al., 2019)	☐	☒	☒	☒	☒	☐	☐	☐	☐
35.	(Peng, Tanguy, et al., 2021)	☒	☒	☒	☒	☒	☐	☐	☒	☒
36.	(Reichle & Koster, 2004)	☒	☒	☒	☒	☒	☒	☐	☐	☐
37.	(Rivera Villarreyes et al., 2014)	☐	☐	☒	☒	☐	☐	☐	☐	☒
38.	(Robinson et al., 2008)	☐	☐	☐	☒	☒	☒	☐	☐	☐
39.	(Scheiffele et al., 2025)	☐	☐	☒	☐	☐	☐	☐	☐	☒
40.	(Schmidt et al., 2024)	☒	☒	☒	☐	☒	☐	☐	☐	☐
41.	(Schrön et al., 2017)	☐	☐	☒	☒	☒	☐	☐	☐	☒
42.	(Senanayake et al., 2021)	☐	☒	☐	☒	☒	☐	☒	☐	☐
43.	(Senyurek et al., 2022)	☐	☒	☐	☒	☐	☐	☒	☐	☐
44.	(Seo et al., 2021)	☐	☒	☐	☒	☐	☐	☒	☐	☐
45.	(Tunçay, 2021)	☐	☐	☐	☒	☒	☒	☐	☐	☐
46.	(Upadhyaya et al., 2021)	☐	☒	☐	☐	☒	☐	☐	☐	☐
47.	(Usowicz et al., 2020)	☒	☒	☒	☐	☒	☐	☐	☐	☐
48.	(Wagner et al., 1999)	☒	☒	☒	☒	☒	☒	☐	☐	☐
49.	(Wang et al., 2021)	☒	☒	☒	☒	☒	☒	☐	☐	☐
50.	(Western & Blöschl, 1999)	☐	☐	☐	☒	☒	☒	☐	☐	☐
51.	(K. Wu et al., 2023)	☐	☒	☐	☐	☒	☐	☐	☒	☐
52.	(B. Xie et al., 2020)	☐	☐	☐	☒	☐	☒	☒	☐	☐
53.	(J. Xie et al., 2025)	☐	☐	☐	☒	☒	☒	☐	☐	☐
54.	(Yan & Bai, 2020)	☐	☒	☐	☒	☒	☐	☒	☐	☐
55.	(Yuan et al., 2020)	☐	☒	☒	☒	☐	☐	☒	☒	☐
56.	(Y. Zhang et al., 2023)	☐	☒	☒	☒	☐	☐	☒	☐	☐
57.	(Zhao et al., 2024)	☒	☒	☐	☒	☐	☐	☒	☒	☐
58.	(Zheng et al., 2009)	☐	☐	☐	☒	☐	☒	☒	☐	☐
59.	(Zheng et al., 2024)	☒	☒	☒	☒	☒	☐	☐	☐	☐
60.	(L. Zhu et al., 2023)	☐	☒	☐	☒	☒	☐	☒	☒	☐